TRANSVERSE HYDRODYNAMICS WITH A FIRST ORDER PHASE TRANSITION IN VERY HIGH ENERGY NUCLEAR COLLISIONS*

BY P. V. RUUSKANEN

Department of Physics, Seminaarinkatu 15, SF-40100 Jyväskylä, Finland

(Received August 25, 1986)

The hydrodynamic treatment of the central region of ultrarelativistic nuclear collisions using the bag model equation of state and assuming a smooth phase transition through equilibrium mixed phase, is reviewed together with the calculation of transverse momentum distributions of hadrons, dilepton spectra and the kinetic evolution of strangeness. Transverse collective flow leads to distinct features in the hadron and dilepton spectra. To study the flow, the events must be sampled according to their multiplicity, which essentially fixes the initial conditions for the flow. The transverse momenta of the hadrons show clear correlations with the equation of state. Boost invariant longitudinal expansion leads to fast cooling of plasma and strong reduction of the average transverse momentum of hadrons. It is argued that the highest values of transverse momenta which are reported from the cosmic ray experiment, are not easily understood to be of thermal origin. Dilepton spectra in the mass range of a few GeV may offer a possibility to get experimental information on the initial temperature of the matter. Strangeness abundance is argued to be insensitive on the initial temperature of the plasma, but may offer a way of determining the critical temperature.

PACS numbers: 25.70.-z, 47.75.+f

1. Introduction

In these lecture notes I will discuss a hydrodynamic scenario [1, 2] for the description of the central region of ultrarelativistic ($E_{cm} > 100$ GeV/nucleon pair) nucleus-nucleus collisions. Hydrodynamics is used to map the space-time evolution of the strongly interacting matter during the collision. Once this space-time history is known, it allows, when supplemented with a decoupling algorithm and appropriate rate equations, the calculation of measurable quantities like hadron spectra, dilepton rates etc. [3–5].

The main motivation in studying very energetic nuclear collisions is the possibility of producing strongly interacting matter at so high energy densities, that it may appear as quark-gluon plasma [6–8]. Theoretical support for the existence of this state of matter

* Presented at the XXVI Cracow School of Theoretical Physics, Zakopane, Poland, June 1–13, 1986.

of deconfined quarks and gluons comes from the lattice QCD calculations [9], which show a rapid increase in energy and entropy density as a function of temperature. In the pure SU(3) gauge theory the transition from hadron gas phase to gluon matter appears to be of first order [9] but with dynamic fermions the studies are still on a preliminary stage and the nature of the transition is not yet clear [10–12].

In the plane of temperature T and the baryon number chemical potential μ_B, the expected phase diagram of hadronic matter is shown in Fig. 1. For a first order transition, the two phases are separated by the curve $p_q(T, \mu_B) = p_h(T, \mu_B)$ on which they can coexist in equilibrium. Regions relevant for different phenomena are indicated in the figure,

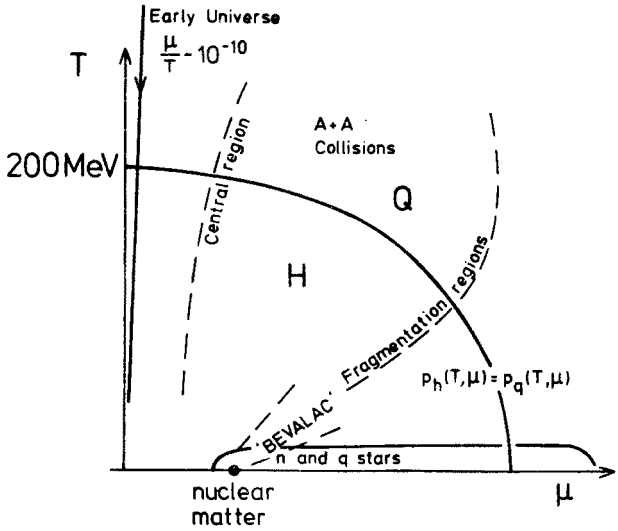

Fig. 1. Phase diagram of strongly interacting matter

perhaps with some degree of optimism in the case of nuclear collisions. At zero chemical potential the transition temperature T_c is estimated to be around 200 MeV both from lattice results and from common sense arguments (e.g. considering the temperature of pion gas at densities where pions start to overlap and fill all the space). I will come to the other parameters when discussing the equation of state.

At first instants of collision copious production of quanta takes place. The production mechanism of matter is badly known and it is of great importance and interest to learn even the gross features of particle production from the coming experiments at CERN and BNL. There are several models for the particle production either based on the phenomenology of hadron-hadron and hadron-nucleus collisions [13, 14] or ideas drawn from QCD [15–19]. They all have the common feature that the colliding nuclei will not stop and turn all their kinetic energy into matter and heat but, instead, will keep on going with a large part of the original baryon number at a rapidity which is a couple of units less than the original rapidity. These remains of the nuclei constitute the fragmentation regions. Between them, in the central region (CR), the production of matter takes place in a proper

time interval τ_0, which may depend on the amount of production [16–19]. If the production is abundant, the produced quanta are quarks, anti-quarks, and gluons which will reach (approximate) thermal equilibrium in time τ_i. The total time for formation and thermalization of matter is expected to be of the order of 1 fm or less in the CR [20–22]. The period of thermalization between τ_0 and τ_i can be studied in terms of kinetic theory [22, 23] but will not be considered here, because from the point of view of the flow it can be included in the initial conditions. From time τ_i on (if ever), hydrodynamics is applicable until the expansion dilutes the matter so much that collisions cease at time τ_{dec} and the particles decouple.

We will see later that the decoupling times are typically few tens of fm. It is clear that due to this rather long period of final state interactions the measured distributions do not directly represent the properties of production dynamics. Even more important, the outcome depends on the properties of the matter during the expansion. As will be shown later, this dependence may lead to correlations between different measurable quantities and so offer a possibility to study the properties of the produced matter in a way which assumes very little knowledge of the production dynamics.

At the moment we are not able to deal with the whole phase space of the produced particles nor with arbitrary collisions. We have assumed central collisions (cylindrical symmetry) of equal size nuclei. We also assume, that at high energies the production in the CR is independent of rapidity. Different observers moving along the collision axis (z–axis) with rapidities confined to CR rapidity interval, will observe identical matter distribution. This invariance in longitudinal Lorentz boosts constraints the form of the solutions severely [24] and makes the hydrodynamic treatment of this part of the phase space a relatively easy task even for matter undergoing a phase transition. Formally our calculations correspond to the limit of infinite collision energy [25].

I will start the more detailed presentation by briefly discussing the equation of state. The hydrodynamics with cylindrical symmetry in the transverse and Lorentz boost invariance in the longitudinal direction is then presented with a few comments on the numerical method [26, 27]. I will then describe the decoupling algorithm for the computation of observable quantities, like particle spectra, from the hydrodynamic variables. The purely thermal densities and distributions are presented as a reference for exhibiting the effects of collective flow. They are also useful in estimating how large errors are caused through the use of massless particle approximation. Before giving the results on observable quantities I shall describe the general features of the flow and its dependence on the initial conditions. Of observables, p_T–distributions and the average values of transverse momenta, $\langle p_T \rangle$, are presented first with special emphasis on how the equation of state affects the correlation between multiplicity and $\langle p_T \rangle$. I will also compare the numerical results of $\langle p_T \rangle$ with the experimental cosmic ray results of the JACEE [28] group and discuss the implications of this comparison. The dilepton spectra are shown to give information on the flow and (possibly and hopefully) on the initial temperature. The last results show how the strangeness might be processed during the evolution and what is its likely outcome in the central region.

Essentially the same scenario has been explored for the p_T–distributions by Blaizot

and Ollitrault [29] using a different numerical method. It is described in the lecture notes of Blaizot [30]. Those results which are common with our calculations and can be compared, agree within the expected numerical accuracy.

2. *Equation of state*

The assumption that hydrodynamics can be applied, means (as a minimum requirement) that thermodynamic concepts can be used to describe the matter. The dynamical properties of the matter are given by the equation of state, which expresses the pressure p in terms of the energy density ε and the conserved quantum number densities like n_B, the net baryon number density. In principle this can be derived from the basic dynamical properties of the quanta of the matter by calculating the partition function. For the strongly interacting matter this can be done presently only in certain limits or numerically in the lattice approximation [9]. Even in the case of purely gluonic matter, when the numerical results indicate rather conclusively a first order transition, the values of the parameters like critical temperature, are not very precisely known, because of uncertainties in connecting the lattice parameters to the physical parameters.

From the point of view of hydrodynamics, even a reliable determination of the equation of state in the thermodynamic limit would not be enough, because it would not tell how the phase transition kinetics works in a rapidly evolving system. If, e.g. the transition is of first order, we would still not know if there is supercooling and associated with it, shock phenomena in the matter, or if the matter evolves through the mixed phase staying all the time close to the thermodynamic equilibrium.

In our scenario we, first of all, assume that in the central region the baryon number density is so small that it can be neglected. The equation of state is then a relation between the pressure p and the energy density ε. The essential feature of all lattice results is the large increase in the energy and entropy densities, possibly at fixed temperature or in a narrow temperature range, the pressure at the same time either staying constant or changing much more slowly. This behaviour is a signal of large increase in the number of degrees

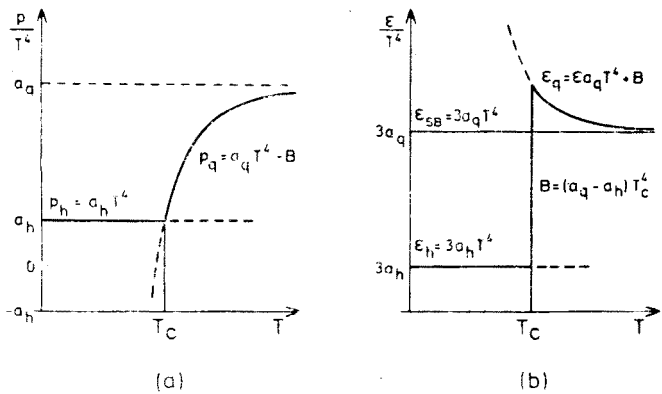

Fig. 2. Pressure and energy density for the bag model equation of state

of freedom in the matter; a feature which one expects if the quark-gluon structure of hadrons is assumed. The next assumption, which cannot be justified, is that the timescales in the phase transition kinetics are short compared to the expansion time scale. If this is true, the precise nature of the phase transition is not likely to be very important for the hydrodynamic evolution of the system. In particular, a second order phase transition with steep increase of ε would differ from a first order transition with comparable jump in ε only in such a way that a space-time region of constant temperature and pressure of the latter would be replaced with a region of slow variation.

Our actual calculations are performed assuming a first order phase transition which we describe with the bag model equation of state treating both phases separately as ideal fluid of noninteracting quanta. Since the parameters must be specified for the numerical calculations and results, the equation of state is exhibited graphically in Fig. 2 with relevant formulae to fix the notation. As basic parameters, we use the number of degrees of freedom

$$\begin{array}{ll} g_h & \text{in hadron phase} \\ g_q = 2 \cdot 8 + n_F \tfrac{7}{8} \cdot 2 \cdot 2 \cdot 3 & \text{in quark} - \text{gluon phase,} \end{array} \tag{2.1}$$

(n_F is the number of flavours) and the bag constant B, which describes the whole complicated dynamics responsible for the phase transition. The critical temperature T_c is determined by the condition $p_h = p_q$ and is related to these parameters through

$$B = (a_q - a_h) T_c^4, \tag{2.2}$$

with $a_i = g_i \pi^2/90$. Other quantities which will be refered to later, are the critical entropy and energy densities

$$\begin{array}{ll} s_H = s_h(T_c) & s_Q = s_q(T_c) \\ \varepsilon_H = \varepsilon_h(T_c) & \varepsilon_Q = \varepsilon_q(T_c), \end{array} \tag{2.3}$$

and the ratio $r_{dof} = g_q/g_h$. In the formulae of Fig. 2, massless quanta in both phases are assumed. The numerical results are for $g_h = g_\pi = 3$ and $n_F = 2.5$ to roughly account for the mass suppression of strange quarks. This gives $r_{dof} = 14.1$. (In cosmological application, also the leptons must be included. This reduces the value of r_{dof}).

It is clear, that this constitutes a very rough representation of the equation of state. However, from the point of view of the reliability of the hydrodynamic results, the assumption on the phase transition kinetics (fast nucleation) is as crucial as the approximations in the equation of state. If the assumption of homogeneous mixed phase holds even roughly we should have a fair amount of hope of getting results which qualitatively and in some cases even semi-quantitatively agree with the true results.

3. Hydrodynamics and the numerical method

The hydrodynamic equations express the conservation of energy and momentum in the fluid by stating that the divergences of the energy and momentum currents vanish [31]:

$$\partial_\mu T^{\mu\nu} = 0, \tag{3.1}$$

where

$$T^{\mu\nu} = (\varepsilon + p)u^{\mu}u^{\nu} + pg^{\mu\nu} \tag{3.2}$$

is the stress-energy tensor for the ideal fluid. The energy density in the comoving frame is ε, p is the pressure and u_{μ} the four velocity of the flow satisfying $u^2 = -1$. In the flow of an ideal fluid, the total entropy is conserved. This follows from Eqs (3.1) and (3.2) and can be written in the form

$$\partial_{\mu}s^{\mu} = 0, \tag{3.3}$$

with

$$s^{\mu} = su^{\mu}, \quad s = (\varepsilon + p)/T,$$

the entropy current and density. For nonzero baryon number density we would also have

$$\partial_{\mu}j^{\mu}_{\mathrm{B}} = 0, \tag{3.4}$$

expressing the baryon number conservation. In this case the pressure would depend both on ε and n_{B} (or T and μ_{B}).

Let us next consider the constraints on the form of the solutions. With cylindrical symmetry there is no dependence on the azimuthal angle ϕ, and we assume that the transverse flow is radial (see, however Ref. [32]). Longitudinal boost invariance means that the whole description of the flow must appear the same in frames boosted in the longitudinal direction (within the CR plateau). In particular, the initial state of the matter can then be specified by going into the longitudinal rest frame of any slice of matter and giving the transverse dependence of the temperature distribution (and other densities if necessary) and the transverse velocity in that slice at the time of thermalization. From the point of view of hydrodynamics the time of thermalization is the initial time and the state of the matter constitutes the initial conditions for the hydrodynamic equations. Since the solutions will satisfy the combined symmetry of the equations and the initial conditions, they will be boost invariant, too.

The appropriate variables in this situation are the longitudinal proper time

$$\tau = \sqrt{t^2 - z^2}, \tag{3.5a}$$

the space-time rapidity

$$\eta = \tfrac{1}{2}\log\left(\frac{t+z}{t-z}\right), \tag{3.5b}$$

and the transverse distance from the collision axis, r. We also use $\hat{t} = \log\tau$. Since τ and r do not change in longitudinal boosts, scalar quantities like temperature or energy density can depend on them but not on η.

In order for the equations to stay form invariant in the longitudinal boosts, the time and longitudinal components of the four velocity of the fluid must be proportional to t and z (with the same factor of proportionality, which can depend on τ and r) and the radial

component can depend on τ and r, alone. This allows us to write u^μ as

$$u^\mu = \gamma_r(\tau, r)\left(\frac{t}{\tau}, v_r(\tau, r), 0, \frac{z}{\tau}\right). \tag{3.6}$$

The condition $u^2 = -1$ gives $\gamma_r = 1\sqrt{1-v_r^2}$. The longitudinal component of the velocity is z/t and the transverse component $(\tau/t)v_r(\tau, r)$ (at $z = 0$, $v_r(t, r)$). Defining the transverse rapidity y_T as

$$y_T = \tfrac{1}{2}\log\left(\frac{1+v_r}{1-v_r}\right), \tag{3.7}$$

u^μ can be written as

$$u^\mu = \cosh y_T(\cosh \eta, \tanh y_T, 0, \sinh \eta). \tag{3.8}$$

In the case of general, cylindrically symmetric flow, u^μ can be written in this form with η replaced by θ, the longitudinal rapidity of the flow. Now, however, both y_T and θ depend on all variables τ, η and r. This is always the situation in the fragmentation regions.

From the above discussion we see that the boost invariance fixes the longitudinal dependence of all quantities and reduces the problem effectively to a $1+1$ dimensional one, for which the equations are easily written down [1, 24]. Once the solution is known at $z = 0$ (or equivalently at $\eta = 0$), it can be boosted to arbitrary $z(\eta)$. Physically the flow is, of course, 3-dimensional and the coupling of longitudinal flow to the transverse flow has a profound effect on the transverse distributions as will be seen from the results.

Without phase transition, e.g. the method of characteristics [33] can be applied to solve the problem numerically [24]. With phase transition the numerical problem becomes more involved. The velocity of sound is zero in the mixed phase making the characteristics to merge and rendering the method of characteristic inapplicable. Also other methods tend to develop instabilities when pressure gradients vanish in some region as we experienced in the connection of numerical calculations of longitudinal expansion [34].

The numerical method which we have employed to integrate the hydrodynamic equations, is a relativistic extension of the so called flux corrected transport (FCT) algorithm invented by Boris and Book [26, 27]. Its special merit is the ability to handle discontinuities in the flow. In our problem, the discontinuities appear as rarefaction shocks [35] at the interphase of hadron gas and quark matter [36–38] or hadron gas and the mixed phase [2] when the matter transversely expands into vacuum. In the smooth scenario which we assume, the surface deflagration from quark phase to hadron gas can occur only for a very brief period before the longitudinal cooling dilutes the matter into the mixed phase.

Conventionally, good accuracy in the numerical integration of differential equations is achieved by using a high order expansion of the equation in terms of finite differences. In the case of steep gradients such an expansion fails. The higher order terms become large and cause extra ripples to the quantities and may finally lead to a blow up of the solution. Low order methods do not suffer as much from the oscillations but they produce extensive numerical diffusion, which tends to smooth out any structure of the solutions. The FCT

algorithm combines a low order algorithm with a high order one in such a way as to keep the best features of both. Basically this is done by using a high order algorithm as much as possible without producing dispersive ripples. Whenever these arise, the step is replaced by a low order algorithm to the extend which is necessary for avoiding the ripples. As a result the algorithm is of no definite order. The general features of the method can be found in Ref. [27] and the practical details for the present problem in Ref. [1].

4. Decoupling algorithm

Decoupling (or freeze out) is the transition of matter from the state of thermodynamic equilibrium with finite pressure to a state of freely streaming particles without pressure. As the matter expands, the densities decrease and the mean free paths increase until they reach the size of the system and become even larger. After this time most particles are not expected to scatter and it should be a good approximation to treat the matter as consisting of free particles. In order to get from the collective flow quantities, like particle density $n(\tau, r)$ and flow velocity $u^{\mu}(\tau, r)$, known from the hydrodynamic calculation, to quantities which describe the distributions of the final particles, like transverse momentum distribution dN/dp_{T}^2, some element of kinetic theory is needed. A simple solution for this link has been proposed by Cooper and Fry [39]. The basic assumption is that up to a certain point the matter evolves as an ideal fluid and from that point on as free particles. Since we know the momentum distribution of particles in the rest frame of any ideal fluid element, we can boost these distributions with the flow velocity and add them up (with proper care because different elements reach the decoupling point at different times) to get the total particle distribution.

In order to understand the insensitivity of this procedure on the precise time of decoupling, consider first a spherically symmetric situation. In this case the average p_{T} (with respect to any fixed direction) is, as a consequence of the symmetry of the flow and conservation of total energy and particle number (entropy), independent of the time of the decoupling, indicating a balance between the flow velocity and the thermal motion. This can be looked at also in terms of the work, which is done by the pressure during the expansion and which turns the random thermal motion into the collective motion. In spherical case the collective motion gains energy with the same rate in all directions, which leads to the constancy of $\langle p_{\mathrm{T}} \rangle$.

The situation is quite different with the strong asymmetry of the initial collective motion for the boost invariant flow considered here. During the early part of the expansion, the flow, and consequently the increase in volume, is almost entirely in the longitudinal direction. Thus, at this stage the thermal energy goes mainly into the longitudinal collective motion [40] resulting in fast decrease of $\langle p_{\mathrm{T}} \rangle$ of the particles. If this would be the situation also at the time of decoupling, the results would be very sensitive to the details of the decoupling. This, however, is not the case as will be argued next.

To determine where the decoupling takes place, one should estimate the mean free paths of quanta and compare them with the size of the system. At $T = 200$ MeV the mean free path in the pion gas with pion cross section of 20 mb is about 1.5 fm and at 100 MeV

about 15 fm. This indicates that the decoupling takes place at fairly low temperatures when a strong flow (for most initial conditions) has been build up also in the transverse direction. In further expansion the situation now resembles that in the spherical case and also the transverse direction gains in collective energy. In our actual calculations a fluid element decouples, when its temperature reaches a specified value, T_{dec}. When T_{dec} is changed from 140 MeV (which has been used to obtain the results below) to 100 MeV, the change of $\langle p_{\mathrm{T}} \rangle$ is less than 2% for $\varepsilon_{\mathrm{i}} > 1$ GeV/fm^3. Clearly other uncertainties, like mass effects, are more important. The effect of the initial asymmetry is clearly seen in the case with $\varepsilon_{\mathrm{i}} = \varepsilon_{\mathrm{H}} = 0.2$ GeV/fm^3. In this case the transverse flow is still quite weak during the time when T drops from 140 MeV to 100 MeV. Longitudinal cooling is then more important and $\langle p_{\mathrm{T}} \rangle$ drops by 10%.

It should be noted, that even in the spherical situation the shape of the momentum distribution does not stay the same. Also, since the hadron gas contains particles with different masses, $\langle p_{\mathrm{T}} \rangle$ would not be conserved separately for each particle species. As will be seen below, the mass of the particles causes a strong correlation between the flow and the p_{T}-distribution [20, 41], leading to a possibility of experimental observation of the flow.

There are of course other uncertainties connected with decoupling, which need further study. First of all, decoupling is not an instantaneous event but takes place gradually. During this stage a non trivial amount of entropy production may take place [42], which can change appreciably the final distributions. To study this, a more involved kinetic treatment covering a finite time interval at the decoupling is necessary [43].

Next we will consider the explicit form of the decoupling integrals. The decoupling condition $T(\tau, r) = T_{\mathrm{dec}}$ determines a three dimensional space-time surface σ, whose surface elements are four vectors denoted by $d\sigma_\mu$. Consider first a current j^μ_Q, which describes the flow of some density like that of the baryon number or strangeness. Then the amount of this quantity passing through the surface element $d\sigma_\mu$ is

$$dQ = j^\mu_Q d\sigma_\mu \tag{4.1}$$

and the total amount which emerges from the collision is obtained by integrating (4.1) over the whole decoupling surface σ. If the decoupling takes place simultaneously in a given spatial region, then $d\sigma^\mu = (d^3\vec{x}, 0, 0, 0)$ (since $dt = 0$) and $dQ = j^0_Q d^3\vec{x}$. In this case the integral of (4.1) simply gives the amount of Q in that region at time t. More generally $d\sigma^\mu$ is of the form

$$d\sigma^\mu = (d^3\vec{x}, dt d\vec{S}). \tag{4.2}$$

The resulting form

$$j^\mu_Q d\sigma_\mu = j^0_Q d^3\vec{x} - dt\vec{j}_Q \cdot d\vec{S} \tag{4.3}$$

can be interpreted (e.g.) as follows: At times t and $t+dt$ the decoupling condition $T(t, \vec{x}) = T_{\mathrm{dec}}$ determines two spatial surfaces, parts of which are illustrated in Fig. 3. The volume part $j^0_Q d^3\vec{x}$ counts the number of particles at fixed instant of time in the layer between the surfaces. However, there is a time difference dt between counting the particles

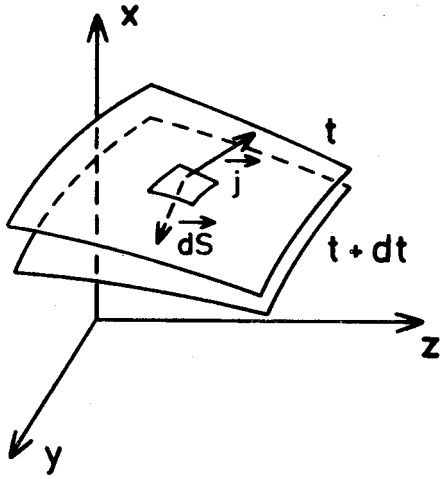

Fig. 3. The spatial decoupling surface at times t and $t+dt$. The surface is defined by the condition $T(t, \vec{x}) = T_{\mathrm{dec}}$ with fixed t

of two adjacent layers. During this time interval particles pass from one layer to the other due to the flow, and depending on the direction of flow with respect to the motion of the decoupling surface, they either are not counted at all or are counted twice by the volume term. This effect of flow, when the decoupling is not simultaneous in different regions, is accounted for by the flux term $-dt\vec{j}_Q \cdot d\vec{S}$.

Particle distributions are obtained by folding the flow with the thermal motion which is described by the Wigner distribution function $f(x, p)$. We can interpret

$$f(x, p)d^3\vec{p}\,\frac{p^\mu}{p_0} \tag{4.4}$$

as the current of particles with momenta in $d^3\vec{p}$. Then

$$dN = \int_\sigma f(x, p)d^3\vec{p}\,\frac{p^\mu}{p_0}\,d\sigma_\mu \tag{4.5}$$

is the total number of particles with momenta in $d^3\vec{p}$. For matter with flow 4-velocity $u^\mu(x)$, the ideal gas distribution function in the fixed frame where u^μ is measured, is

$$f(x, p) = \frac{g}{(2\pi)^3}\,\frac{1}{e^{u\cdot p/T} \mp 1}\,,$$

where g counts the number of degrees of freedom and $-$ $(+)$ sign refers to bosons (fermions). The complete form of the invariant momentum distribution is then

$$\frac{dN}{d^3\vec{p}/E} \equiv \frac{dN}{dyd^2\vec{p}_{\mathrm{T}}} = \frac{g}{(2\pi)^3}\int_\sigma f(x, p)p^\mu d\sigma_\mu. \tag{4.6}$$

With our decoupling condition $T = T_{dec} = constant$. For a more general situation, as in the fragmentation region, the baryon number chemical potential must be included in the distribution function and the decoupling condition will depend both on temperature and chemical potential which will vary along the decoupling surface.

With cylindrical symmetry the decoupling surface element can be written as

$$d\sigma^\mu = (rd\phi drdz, \boldsymbol{e}_r rd\phi dzdt, 0, \boldsymbol{e}_z rd\phi drdt), \tag{4.7}$$

and the flow velocity in the form (3.8) with the space-time rapidity η replaced by the longitudinal flow rapidity θ (see the text after Eq. (3.8)). We can use $\vec{p}_T$ to fix the direction of x–axis in the transverse plane. Then

$$p_\mu u^\mu = m_T \cosh y_T \cosh(\theta - y) - p_T \sinh y_T \cos\phi \tag{4.8}$$

and

$$p^\mu d\sigma_\mu = rd\phi d\eta(m_T\tau \cosh(\eta - y)dr + m_T \sinh(\eta - y)d\tau - p_T\tau \cos\phi d\tau), \tag{4.9}$$

where $m_T = \sqrt{m^2 + p_T^2}$ is the transverse mass and y the rapidity of a particle with momentum p^μ. For the boost invariant flow $\theta = \eta$, and the second term of (4.9) drops out from expression (4.6) in the integration over η, leading to

$$\frac{dN}{dyd^2\vec{p}_T} = \frac{g}{(2\pi)^3}\int_\gamma \tau r \int_0^{2\pi} d\phi \int_{-\infty}^{+\infty} d\eta \frac{m_T \cosh(\eta - y)dr - p_T \cos\phi d\tau}{e^{(m_T \cosh y_T \cosh(\eta - y) - p_T \sinh y_T \cos\phi)/T} \mp 1}. \tag{4.10}$$

Since y is present in the combination $\eta - y$ only, the result is independent of y as it should for the boost invariant situation. Integration over τ and r is along the curve γ defined by the decoupling condition $T(r, \tau) = T_{dec}$. The integrations over η and ϕ can be carried out if we expand the distribution function in geometric series. The result is

$$\frac{dN}{dyd^2\vec{p}_T} = \frac{g}{2\pi^2}\int_\gamma \tau r \sum_{n=1}^{\infty} (\pm 1)^{n+1} \left\{ m_T I_0\left(n\frac{p_T}{T}\sinh y_T\right) K_1\left(n\frac{m_T}{T}\cosh y_T\right) dr \right.$$

$$\left. - p_T I_1\left(n\frac{p_T}{T}\sinh y_T\right) K_0\left(n\frac{m_T}{T}\cosh y_T\right) d\tau \right\}, \tag{4.11}$$

where I's and K's are Bessel functions. The remaining integral is easily done numerically. The result shows explicitly, that the knowledge of transverse flow at $z = 0$ is all what is needed for the calculation of particle spectra in the boost invariant case.

In the fragmentation regions, where boost invariance does not hold, the ϕ-integration can still be done. The remaining 2-dimensional integration will not be the most tedious part of a calculation, which treats simultaneously the transverse and the longitudinal flow in the fragmentation regions.

5. *Thermal distributions*

As an exercise let us apply the decoupling integral (4.11) to the case of no transverse flow, $y_T = 0$. This gives us the p_T–distributions for purely thermal motion and we can use the results later as a reference for the full results.

Since $I_0(0) = 1$ and $I_1(0) = 0$, the decoupling integral simplifies into the form

$$\frac{dN}{dyd^2\vec{p}_T} = \frac{g}{2\pi^2}\int_0^{R_A} dr\tau r \sum_{n=1}^{\infty} (\pm 1)^{n+1} m_T K_1\left(n\frac{m_T}{T}\right). \tag{5.1}$$

For constant T the sum with Bessel functions is independent of the integration and the remaining integral gives the volume per unit rapidity of the matter at decoupling (τ gives the length per unit rapidity at $y = 0$):

$$\left(\frac{dV}{dy}\right)_{\text{dec}} = 2\pi \int_0^{R_A} dr\tau r. \tag{5.2}$$

The final form of the distribution is

$$\frac{dN}{dyd^2\vec{p}_T} = \left(\frac{dV}{dy}\right)_{\text{dec}} \frac{g}{4\pi^3} m_T \sum_{n=1}^{\infty} (\pm 1)^{n+1} K_1\left(n\frac{m_T}{T}\right). \tag{5.3}$$

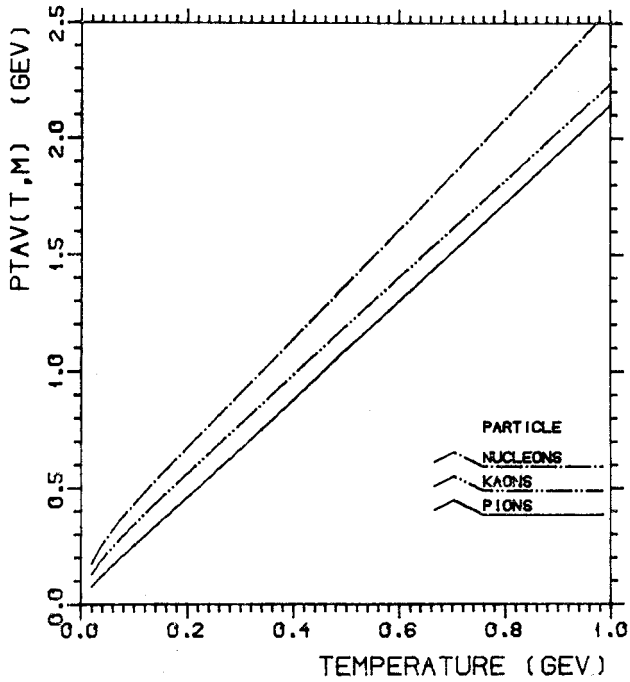

Fig. 4. Average thermal transverse momenta of pions, kaons and nucleons as a function of temperature

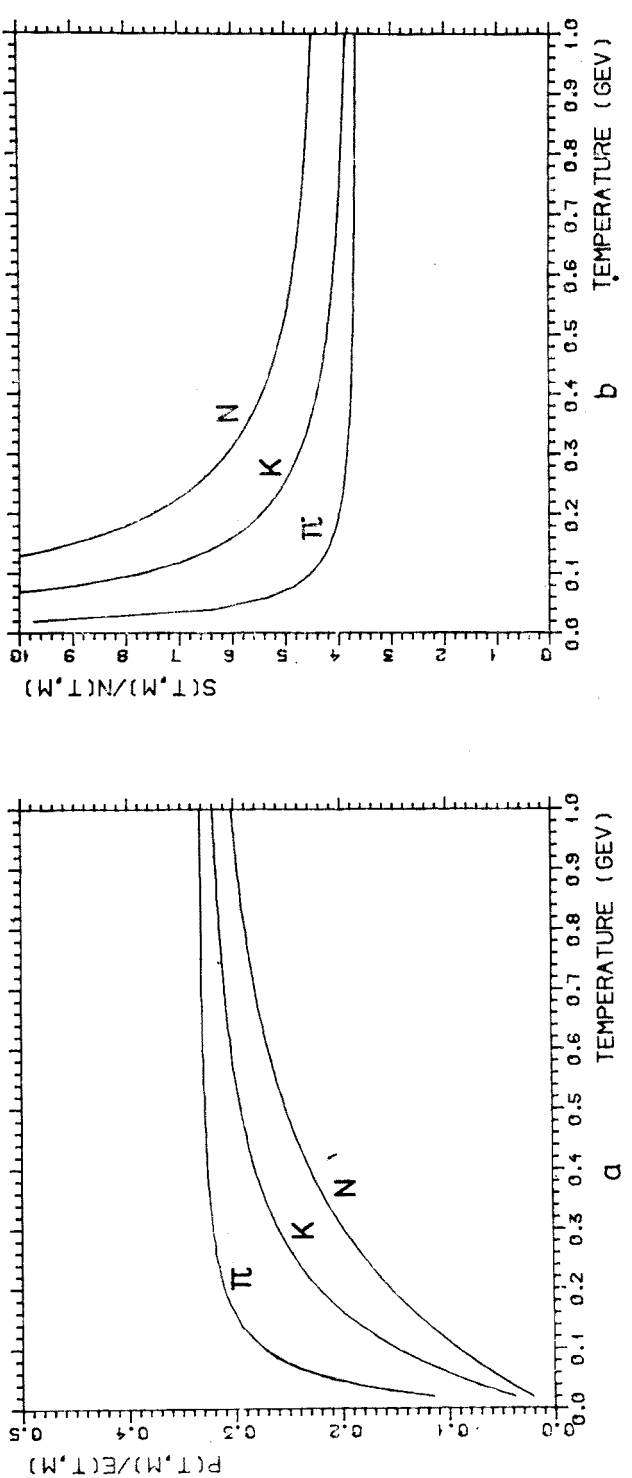

Fig. 5. The ideal gas ratios of pressure to energy density and entropy to number density for pions, kaons and nucleons as function of temperature T

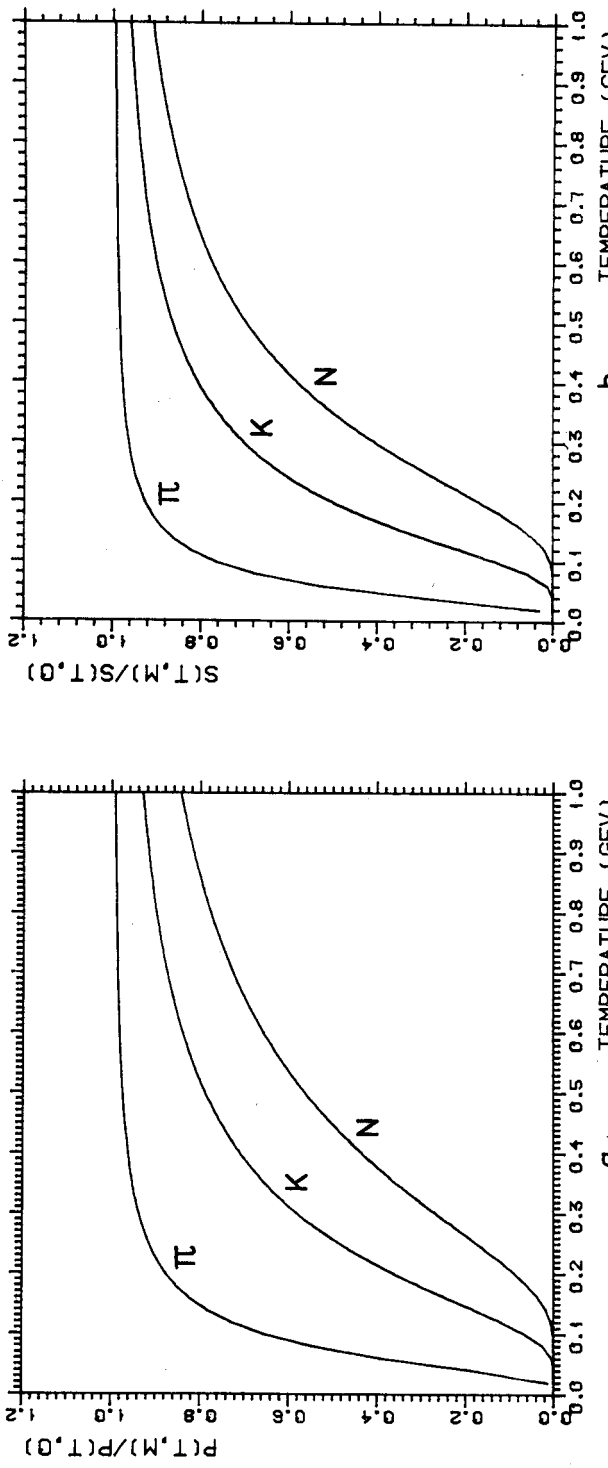

Fig. 6. Mass dependence of the pressure and the entropy density of an ideal gas is illustrated by showing their ratio to the corresponding quantities for massless quanta

which is the "official" [44] thermal distribution. The thermal particle density n is obtained by integrating over p_T and dividing out the volume. The average value of p_T is

$$\langle p_T \rangle = \sqrt{\frac{\pi m T}{2}} \frac{\sum_{n=1}^{\infty} \frac{1}{n^{3/2}} (\pm 1)^{n+1} K_{5/2}\left(n \frac{m}{T}\right)}{\sum_{n=1}^{\infty} \frac{1}{n} (\pm 1)^{n+1} K_2\left(n \frac{m}{T}\right)}. \tag{5.4}$$

For massless particles these simplify to

$$\langle p_T \rangle = \frac{3\pi}{4} \frac{\zeta(4)}{\zeta(3)} T \simeq 2.12T, \quad \text{bosons}$$

$$= \frac{3\pi}{4} \frac{\eta(4)}{\eta(3)} T \simeq 2.47T, \quad \text{fermions} \tag{5.5}$$

where ζ is the Riemann zeta function and $\eta(n) = (1-2^{1-n})\zeta(n)$.

The mass effect in the thermal distributions is shown in terms of $\langle p_T \rangle$ in Fig. 4, where the thermal $\langle p_T \rangle$ of pions, kaons and nucleons is drawn as a function of temperature. We will see below, that the flow leads to much more profound mass dependence of the p_T-distributions.

The expressions of the pressure, energy density and entropy density for massive particles in the ideal gas approximation are well known and need not be written down here. As a useful reference for rough estimation of mass effects, the pressure to energy density and entropy to number density ratios (with $\mu_B = 0$ for nucleons), which are constant in the massless limit are depicted in Fig. 5 for pions, kaons, and nucleons. The ratio of pressure and entropy with physical mass to the same quantity for massless particles is shown in Fig. 6.

6. *Initial conditions and their effect on flow*

The initial conditions at $z = 0$ are given by specifying $T(\tau_i, r)$ and $v_r(\tau_r, r)$, the temperature and radial velocity at τ_i which is the time when (approximate) thermal equilibrium is reached. To determine the initial conditions one would need a reliable model of production, followed by a kinetic treatment of thermalization. A summary of what is presently known about τ_i and T_i, like their scaling with mass number A, is presented in Ref. [30]. I note here only that, e.g. on the basis of the colour flux-type models of production [15], it seems plausible that τ_i and T_i are inversely proportional [16–19];

$$\tau_i = \frac{C}{T_i}. \tag{6.1}$$

This follows from production time being proportional to $1/\sqrt{E_0}$, where E_0 is the strength of the colour field, and from the argument [17, 19] that the distribution of the produced

particles is close to the thermal distribution and thus the thermalization time is essentially the production time. Since the production rate per unit volume $\sim E_0^2$, the initial density of the produced quanta ($\sim T_i^3$ in terms of temperature) will be $n \sim \tau_i E_0^2 \sim E_0^{3/2}$. Putting together these results, gives the relation (6.1). From uncertainty arguments $C > 1$ for the hydrodynamics to make sense. We have used $C = 250$ fm MeV in our actual calculations. This is not important from the point of view of the flow itself as I will explain below, but it will limit, for a given multiplicity, the earliest possible time and maximum T_i and this may have consequences for the dilepton emission.

In the main part of the numerical calculations we have taken $T(\tau_i, r) = T_i$ within the nuclear radius R_A and zero outside. The radial velocity is taken to be zero initially. We have checked the sensitivity of the results on these assumptions by considering smooth temperature distributions and non zero radial velocities. Both effects increase the transverse flow but do not change the results qualitatively. (For details see Refs [3] and [4].)

It turns out that the final flow depends only weakly on τ_i and T_i separately. The essential quantity is the product $\tau_i T_i^3$, which (together with R_A) gives the total initial entropy of the collision. This can be understood by recalling, that in the longitudinal expansion without transverse flow, τT^3 remains a constant [25]. Starting with different τ_i and T_i but the same value of $\tau_i T_i^3$ means that the transverse flow is neglected during $\delta\tau_i$, the difference of the two choices of the initial time. However, as long as $\delta\tau_i$ is small compared to the time-scale of the buildup of the transverse flow, $R_A/v_s \simeq 10$ fm, this will not be important.

In the ideal fluid approximation entropy is conserved and $\tau_i T_i^3$ can be expressed in terms of the multiplicity of the collision as

$$\frac{dN}{dy} = \pi R_A^2 \frac{4a_q}{c} \tau_i T_i^3, \tag{6.2}$$

with $c \simeq 3.6$. This is nice because it allows us to relate the badly known initial conditions to a directly measurable quantity dN/dy. Since the hydrodynamic calculation together with the decoupling algorithm correlates the initial conditions with the final particle distributions, we end up of having correlations between quantities, which can be measured. Large fluctuations in the multiplicity distribution would be very helpful. By sampling the events according to their multiplicity, it would be possible to study how the flow evolves as the initial densities increase. Without such sampling events with different flow patterns will be superimposed and the information on flow is lost.

For signals which depend on the whole history of the matter, like dilepton and photon emission, the time interval $\delta\tau_i$ in the above discussion can be extremely important. The reason is, that the emission rates depend very strongly on temperature. Consequently, the emission during $\delta\tau_i$ can (especially for large masses) dominate the signal. This may offer a possibility to get rather direct experimental information on T_i.

Let us first have a qualitative survey of the characteristic features of the flow. Fig. 7a shows a snapshot of the collision at time 6 fm after the nuclei met in terms of z and r. (See the lecture notes by Blaizot, Ref. [30], for the various regimes of the collision in terms of z and t.) The figure corresponds to actual numerical results with initial temperature

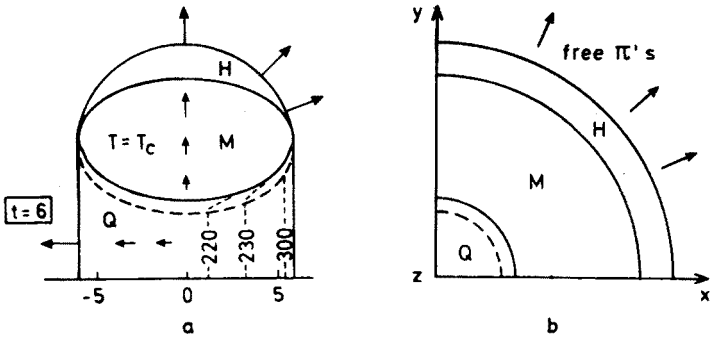

Fig. 7. A snapshot of the flow at $t = 6$ fm in uranium-uranium collision

$T_i = 500$ MeV at time $\tau_i = 0.5$ fm. As the matter is diluted both by the longitudinal and the transverse expansion, several coaxial cylindrical shells with distinct physical features will form. These are illustrated at $z = 0$ in Fig. 7b. For high enough initial energy density, the innermost region consists of plasma, transversally at rest. A rarefaction wave (dashed line) propagates with velocity of sound, $v_s = 1/\sqrt{3}$, into the plasma which is cooled to critical temperature. Further rarefaction leads to the formation of mixed phase region (M). The assumption that the system is able to evolve through equilibrium mixed phase has important implications for the transverse flow. In the mixed phase pressure stays constant, the velocity of sound vanishes, and the ordinary rarefaction wave cannot propagate. Instead, at the interface of the mixed phase and the hadron gas, a shock front develops [2]. The fact that the entropy density of the mixed phase is well above the entropy density of the hadron gas for the main part of the evolution and that the entropy current cannot decrease has two consequences: the velocity of the shock front v_{sh} will be small as compared to the velocity of the ordinary rarefaction wave and there is a sharp jump in the velocity of the matter as the hadron gas must flow out from the shock front with high velocity in order to be able to transport away the entropy of the mixed phase. The velocity of the hadrons relative to the mixed phase, v_h, and v_{sh} are shown for 1-dimensional flow in Fig. 8 as a function of the hadron fraction h defined by

$$s = (1-h)s_Q + hs_H. \tag{6.3}$$

The fast increase of the transverse velocity leads to a rapid drop in the density of the hadron gas and the hadrons decouple quite soon after the shock (the outermost line in Fig. 7).

As is seen from Fig. 7 the longitudinal expansion has cooled also the inner part of the matter at $z = 0$ almost down to the critical temperature T_c. Without transverse flow this happens [25] at

$$\tau_Q = \tau_i \left(\frac{T_i}{T_c}\right)^3. \tag{6.4}$$

If $\tau_Q \ll v_s R_A$, the ordinary rarefaction wave has little effect and the transverse cooling is due to the slowly propagating rarefaction shock. As a result the life time of the inner

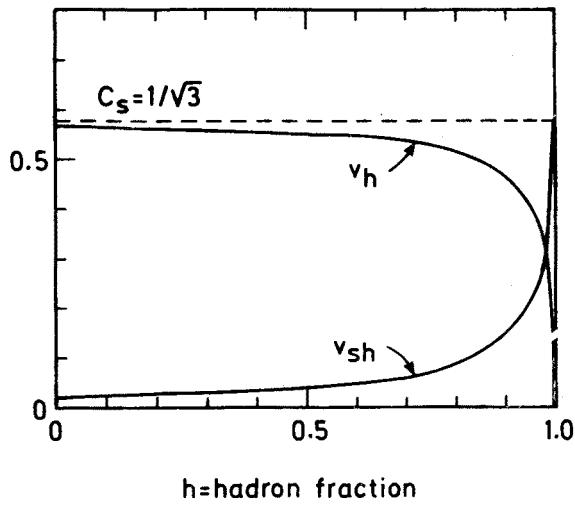

Fig. 8. Velocity of rarefaction shock front, v_{sh}, propagating into the mixed phase with hadron gas fraction h. The curve marked with v_h shows the velocity of the outcoming hadron gas relative to the mixed phase

part of the matter is essentially fixed by the longitudinal cooling and is

$$\tau_H = \tau_Q \frac{s_Q}{s_H} = r_{dof}\tau_Q \tag{6.5}$$

for the mixed phase. After this, all the matter is in the form of hadron gas, which freezes out quite rapidly because the expansion is now three dimensional.

Next I will describe how the flow evolves as the initial temperature T_i or equivalently the multiplicity is increased. The flow figures 9 and 10 are for uranium-uranium collisions with $R_A = 6.8$ fm. The critical temperature has the value $T_c = 200$ MeV, giving for B, ε_H, and ε_Q the values 0.9, 0.2, and 3.7 GeV/fm^3, respectively.

Below the phase transition with $\varepsilon_i \leqslant \varepsilon_H$ (for uranium $(dN/dy)/A \leqslant 0.3$) the flow can be solved analytically; exactly in one dimension and approximately in the case of cylindrical symmetry and boost invariance [24, 2]. The solution, the Riemannian simple wave, proceeds into the matter with the velocity of sound, which for the ideal fluid is $v_s = 1/\sqrt{3}$. The resulting timescale of transverse cooling is $\simeq \sqrt{3}R_A \simeq 10$ fm for large nuclei. For $T_{dec} = 140$ MeV, the decoupling condition is always reached, due to the longitudinal expansion, at a time which is short compared to this transverse time scale. This means that the transverse flow is weak and $\langle p_T \rangle$ of hadrons is almost independent of T_i or equivalently of multiplicity.

When $\varepsilon_H > \varepsilon_i > \varepsilon_Q$, corresponding to the multiplicity interval $0.3 < (dN/dy)/A < 4$ for uranium, the matter starts in the mixed phase. As mentioned above, the rarefaction proceeds into the mixed phase as a discontinuity which becomes stronger as ε_i grows towards ε_Q. The time for the shock front to propagate into the matter increases, too, leading to an overall growth of the transverse flow. There is a small amount (maximum

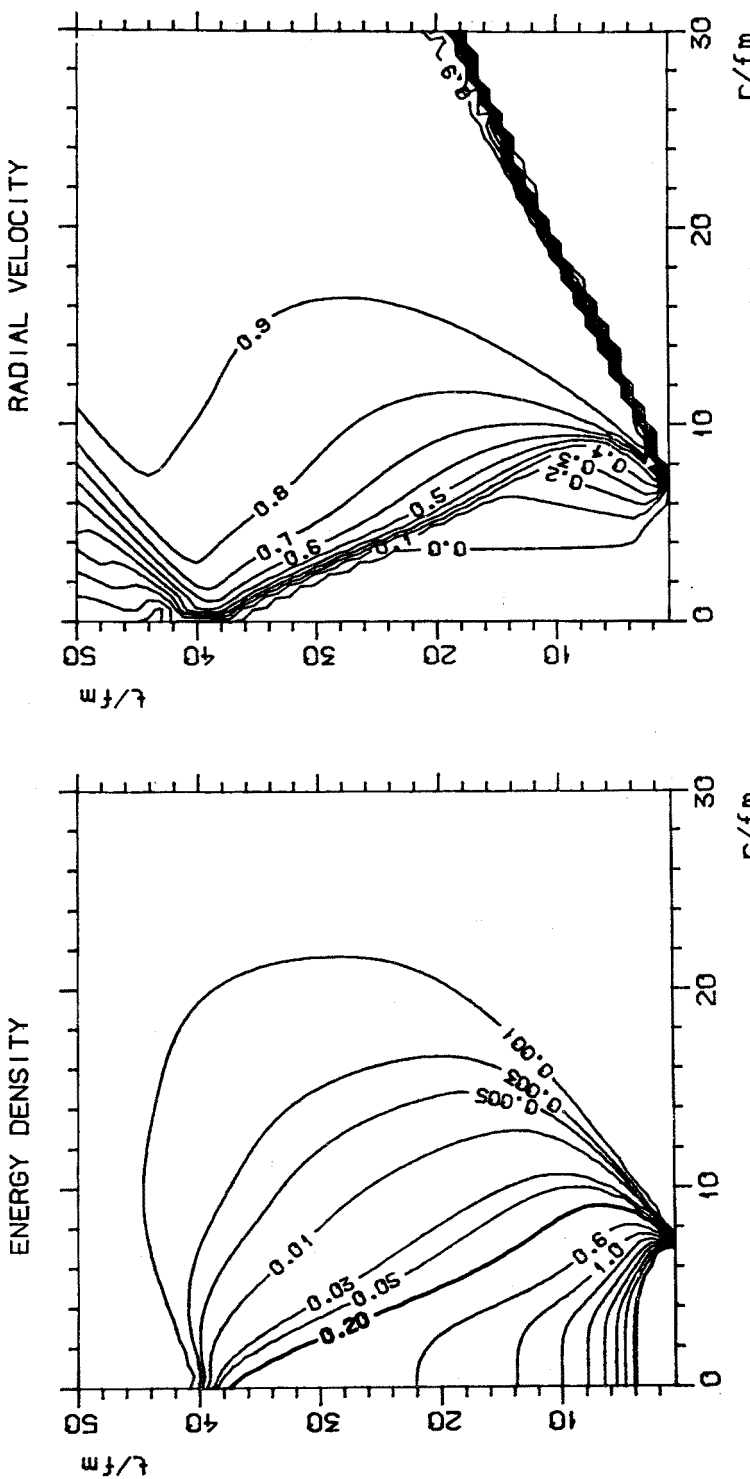

Fig. 9. Curves of constant (a) energy density in units of GeV/fm^3 and (b) transverse velocity for a flow with $\varepsilon_i = \varepsilon_Q$, plotted in the plane of proper time ($t$here t) and radial distance r. The mixed phase lies between the thicker curves with $\varepsilon = \varepsilon_Q = 3.6$ and $\varepsilon = \varepsilon_H = 0.20$.

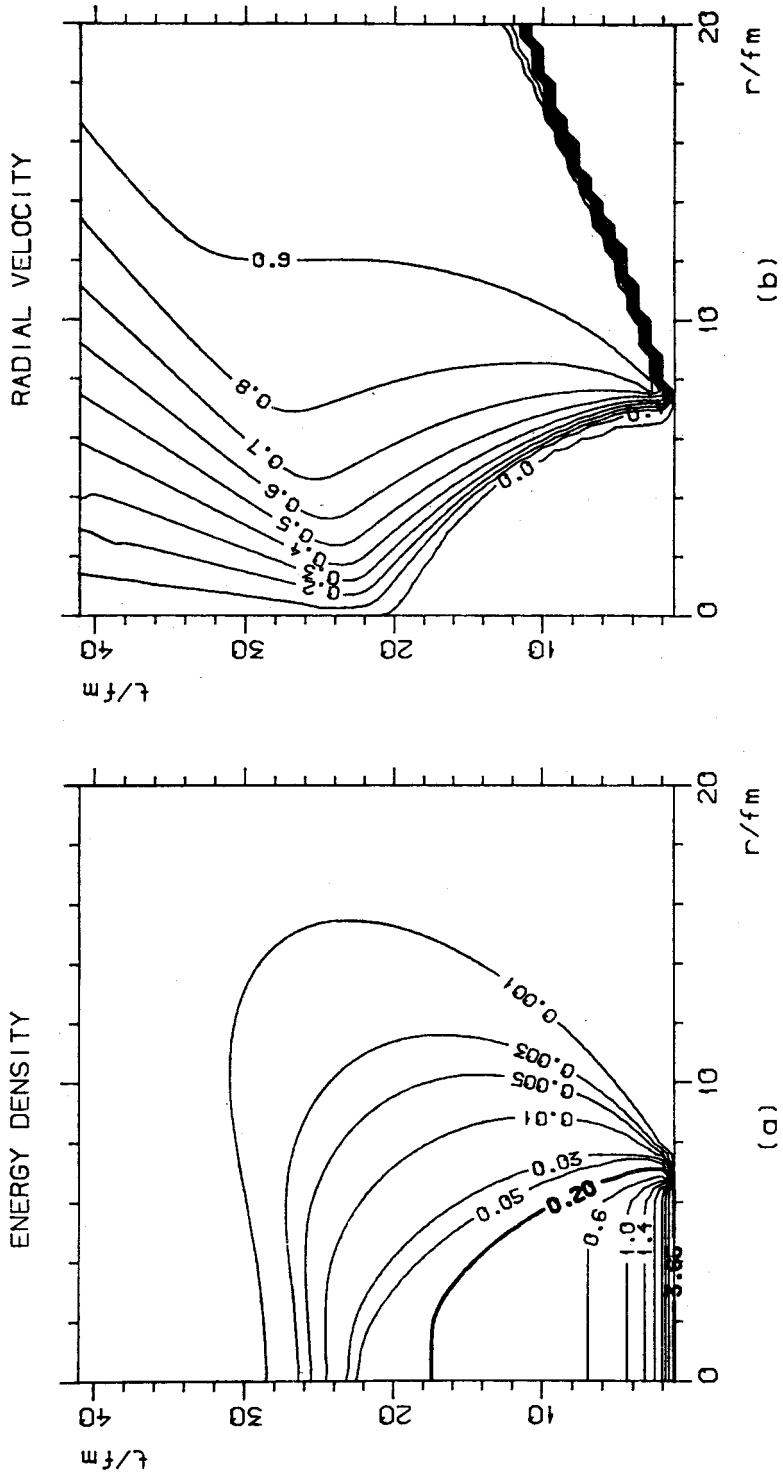

Fig. 10. Same as Fig. 9 but for $T_i = 350$ MeV at $\tau_i = 0.7$ fm

$\sim 7.5\%$) of entropy production at the discontinuity. The complete history of the flow is shown in Fig. 9 for $\varepsilon_i = \varepsilon_Q$ as contour plots of ε and v_r in the rt-plane. All the main features of the flow can be easily seen. The boundary between the mixed and hadron phases is the thick line with $\varepsilon = 0.2$ GeV/fm^3. Inside it matter is at rest and the energy density drops due to the longitudinal cooling with a rate which is independent of r. In the beginning when the density is high, the shock front, which coincides with the $\varepsilon = 0.2$ GeV/fm^3 line and is more clearly seen as a jump in velocity, propagates slowly, but as the longitudinal expansion dilutes the density, the shock gets faster (the bending of $\varepsilon = 0.2$ GeV/fm^3 line) as is seen from Fig. 8. The shock does not reach the collision axis before $t \simeq 17.5$ fm, when the mixed phase is transformed into hadrons by the longitudinal motion alone. The decoupling temperature 140 MeV corresponds to an energy density $\varepsilon = 0.05$ GeV/fm^3, and it is seen that decoupling takes place very soon after the hadrons emerge from the shock.

Further increase in ε leads to a situation where the ordinary rarefaction moves into the quark matter. As long as τ_Q is short compared to $\sqrt{3}R_A$, this is not very important because at that time the temperature drops to T_c, the propagation of the rarefaction wave stops, and the situation becomes similar to that with $\varepsilon_i = \varepsilon_Q$. In this range of initial conditions (which in terms of $(dN/dy)/A$ is not negligible) the strength of the transverse flow grows very slowly.

When τ_Q becomes clearly longer than 1 fm the strength of the transverse flow starts to grow again, the rarefaction wave now being the mechanism of the growth. Fig. 10 shows the flow for $(dN/dy)/A = 13.5$, corresponding to $T_i = 350$ MeV at $\tau_i = 0.7$ fm and $\tau_Q \simeq 4$ fm. The new feature compared to Fig. 9, is the ordinary rarefaction wave which is very clearly seen in Fig. 10b to propagate until time τ_Q. Part of the mixed phase will now be moving transversally. From here on the transverse flow increases rapidly with multiplicity. All the above features of the flow are reflected in a transparent way in the p_T-distributions of hadrons.

7. Transverse momenta of final hadrons

Transverse momentum distributions for pions (massless) are shown in Fig. 11 as a function of multiplicity for uranium-uranium collisions together with thermal distributions (dashed lines). Temperature and normalization of thermal distributions is chosen to give the same $\langle p_T \rangle$ and multiplicity as obtained from the actual calculation with flow. The distributions do not exhibit any dramatic features. For massive particles the situation is different, however [20, 41], because they will gain more momentum from the collective motion than the light pions.

To see the coupling of the mass to the collective flow quantitatively, we have used also for kaons and nucleons the decoupling integral (4.11). Strictly speaking this is not consistent because kaons and nucleons have not been included in the equation of state. For the hydrodynamics the effect in the central region is probably not important. First of all the hadron phase is only a small part of the whole hydrodynamic stage. Second, the density of nucleons and antinucleons is very small (see Fig. 6) and they do not contribute

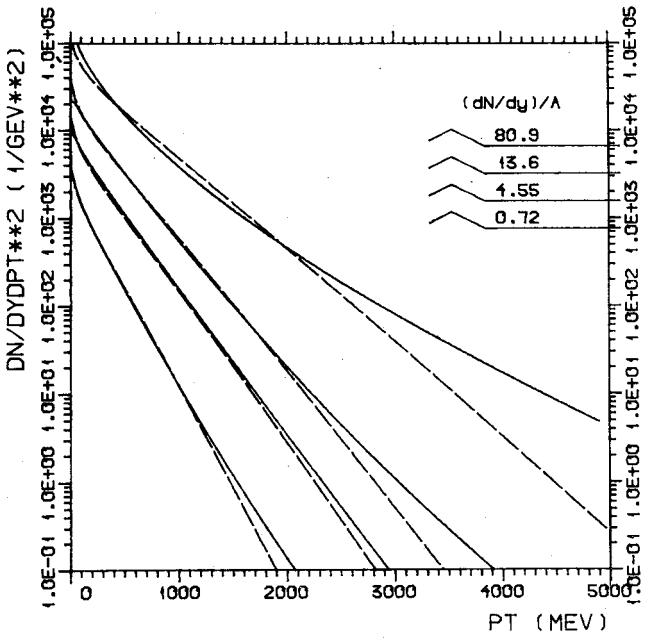

Fig. 11. Transverse momentum distributions of massless pions for different multiplicities. The dashed lines are thermal distributions with temperature fixed to give the corresponding $\langle p_T \rangle$

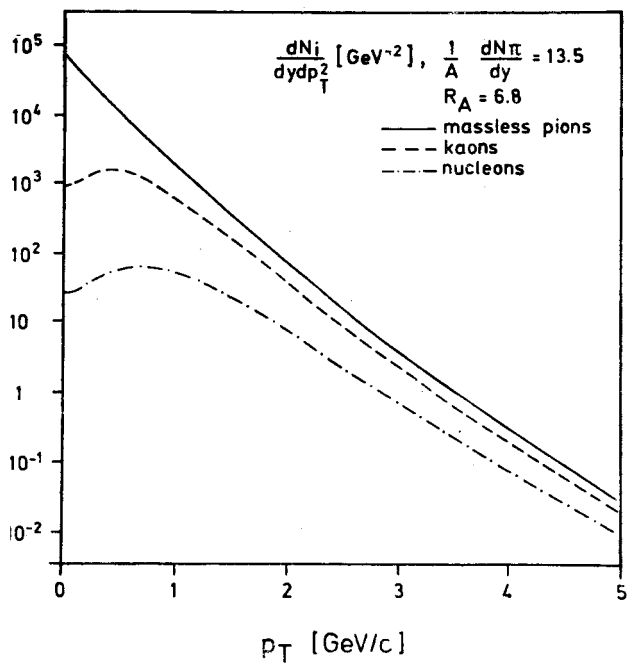

Fig. 12. Transverse momentum distributions of pions (massless), kaons and nucleons showing the effect of mass on the shape of the distributions

much to the energy density or pressure. The amount of kaons can be $\sim 30\%$ (see Fig. 6) and their pressure to energy density ratio deviates from the massless value $\sim 30\%$ (Fig. 5). This would mean $\sim 10\%$ effect to the equation of state. One would not then expect large changes to the flow due to inclusion of kaons and nucleons. The absolute values of separate results should not be taken too seriously; what is more important is the qualitative difference of shapes of p_T–distributions and of the average p_T–values of different particles. Fig. 12 exhibits how the shape depends on the mass of the particle, showing clearly how the flow boosts the heavy particles to high momenta. In terms of $\langle p_T \rangle$ the effect is shown in Fig. 13. The particle mass has an effect on the purely thermal distributions, too, but as

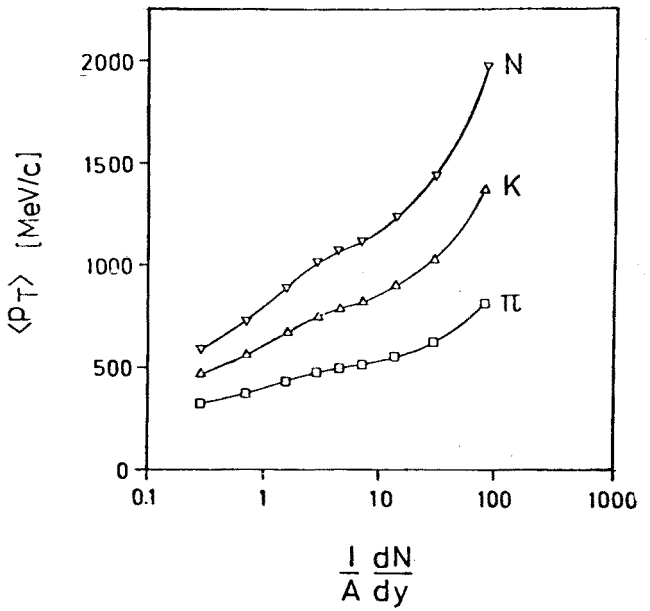

Fig. 13. Average transverse momentum of pions (massless), kaons and nucleons as function of multiplicity

seen in Fig. 4, the differences of $\langle p_T \rangle$ are relatively small compared to the situation with flow. Comparison of Figs 4 and 13 shows explicitly of flow as advocated by McLerran [20] and Shuryak [41]. The experimental observation of large differences in $\langle p_T \rangle$ of pions, kaons and nucleons, growing with multiplicity, would be a strong indication of the existence of the flow.

In the case of heavy particles also the shapes of the spectra clearly differ from the thermal shapes. This is shown for nucleons in Fig. 14 for different initial conditions. For small values of $(dN/dy)/A$ the flow is weak and the distribution is essentially the thermal one. As the flow builds up, the small transverse momentum region is depleted. Observation of these changes of shape would again lend strong support for the existence of collective motion.

All the results above refer to calculations with the bag model equation of state and the phase transition proceeding through equilibrium mixed phase. To see the effect of the

equation of state on the particle distributions, we performed calculations assuming that the matter is always in the form of massless pions. The difference of the two cases is illustrated in Fig. 15 where the average transverse momenta of the pions are plotted as a function of multiplicity. The difference in $\langle p_T \rangle$ comes from the fact that in order to obtain the same multiplicity with pions as with plasma, the initial temperature must be raised by a factor of $\sqrt[3]{r_{dof}} \simeq 2.4$.

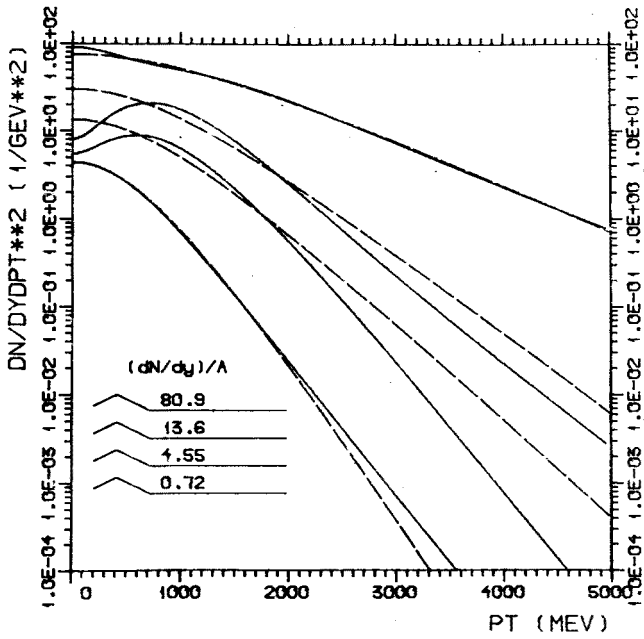

Fig. 14. As Fig. 11, but for nucleons

Earlier I emphasized that the flow depends essentially on $\tau_i T_i^3$ only. This holds for a fixed nuclear radius R_A. We can define a dimensionless initial parameter as [29, 30] $(\tau_i/R_A)(T_i/T_c)^3$, which is easily shown to be proportional to $(dN/dy)/A$. In Fig. 16, $\langle p_T \rangle$ is plotted for different nuclei showing a rough scaling of the results.

Let me next comment on the shape of the $\langle p_T \rangle$ as a function of initial conditions. Usually the existence of the first order phase transition is argued to show up in the dependence of $\langle p_T \rangle$ on initial conditions in such a way that it reflects rather directly the initial temperature of the matter. Thus, in hadron phase, $\langle p_T \rangle$ presumably grows until the transition temperature is reached, it then stays constant as the initial energy density increases across the mixed phase region with constant temperature, and finally starts to increase again when initial energy densities are high enough for the plasma formation. If hydrodynamic expansion really takes place, these arguments have to be refined and in the present picture the behaviour which is described above may be weakened so much, that it cannot be observed. The reason is simply the longitudinal cooling. For matter initially in the hadron phase, $T_i \leqslant T_c$, the transverse flow will be weak and the measured $\langle p_T \rangle$

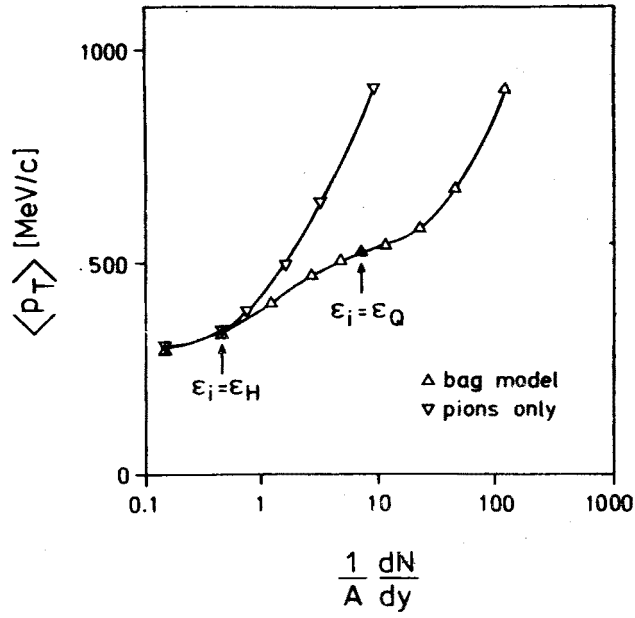

Fig. 15. The effect of the equation of state on $\langle p_T \rangle$ of pions

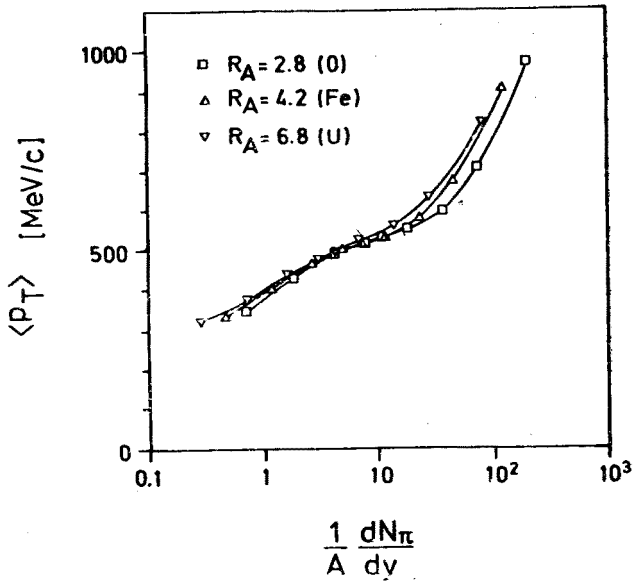

Fig. 16. Approximate scaling of $\langle p_T \rangle$ as a function of $(dN/dy)/A$

is given just by the decoupling temperature T_{dec} and is roughly constant. In Fig. 15 the initial matter is in the hadron gas phase between the first two points, which correspond to $T_i = T_{dec} = 140$ MeV and $T_i = T_c = 200$ MeV, respectively. Between the points, which are indicated by ε_H and ε_Q the initial matter is in the mixed phase and $T_i = T_c = 200$ MeV throughout. Contrary to the naive expectations, $\langle p_T \rangle$ grows in this region. One way to understand this is in terms of the transverse flow, which now has more and more time to evolve before the hydrodynamic expansion dilutes the matter to freeze out. Basically the growth is fed by the vacuum energy expressed by the bag constant B; in plasma at T_c the energy per degree of freedom is roughly 4/3 times the energy per degree of freedom in hadron gas at T_c. As the initial energy density increases, the fraction of plasma increases and so does the overall average energy per degree of freedom. This growth is reflected as a growth of final $\langle p_T \rangle$ via the buildup of the transverse flow.

The flattening of $\langle p_T \rangle$ around ε_Q may look surprising at first. The reason is actually the same as below ε_H. As long as the initial state is such that $\tau_Q \ll v_s R_A$, the longitudinal cooling drops the matter to critical temperature before the ordinary rarefaction wave becomes significant and then the transverse flow evolves as in the case $\varepsilon_i = \varepsilon_Q$ (except for a small difference due to the increase of timescale in longitudinal expansion of mixed phase). When τ_Q becomes comparable with $v_s R_A$, the ordinary rarefaction wave leads to a strong transverse flow already during the plasma and the final $\langle p_T \rangle$ starts to grow. However, the region of growth corresponds to very large multiplicities (note the logarithmic scale) or initial energy densities as I will point out next by considering the results together with the JACEE data.

8. Thermal origin of large $\langle p_T \rangle$'s and the JACEE data

The data on average transverse momenta in nuclear collisions as measured by the JACEE group in a cosmic ray experiment [28] is shown in Fig. 17 together with the results from the hydrodynamic calculation. The abscissa, $\tilde{\varepsilon}_i$, is a measure of the initial energy density at time $\tau = 1$ fm and is calculated from the formula [28]

$$\tilde{\varepsilon}_i = \sqrt{p_T^2 + m_\pi^2}\, \frac{3}{2} \frac{dN_{ch}}{dy} \frac{1}{V}, \tag{8.1}$$

with $V = 2\pi A^{2/3}$, the initial volume per unit rapidity at $r = 1$ fm. Only those data points are included, where both colliding systems are nuclei. The curves are constructed from the hydrodynamical results using the same formula. The dashed curve corresponds to pure pion gas and the continuous curves to the bag model equation of state. The mass value of the colliding nuclei is taken to be 56 ($R_A = 4.2$ fm) in the calculations. This is larger than the average A of the smaller nucleus in the JACEE data, but in the calculation the dependence on A is weak.

It is clear that the calculation with bag equation of state does not reproduce, what is usually interpreted as a break in the data. However, one should be careful in interpreting the shape of the data. If the two highest points are removed, the break more or less disap-

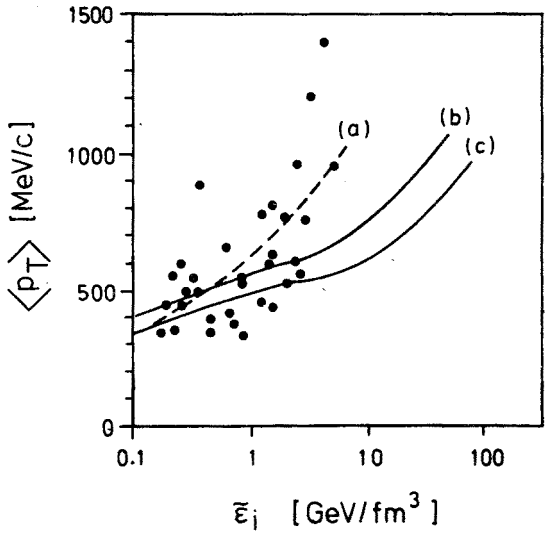

Fig. 17. JACEE cosmic ray data and the numerical results: (*a*) massless pion gas, (*b*) bag equation of state with $m_\pi = 140$ MeV at decoupling and (*c*) bag equation with massless pions

pears and the $\langle p_T \rangle$ appears to increase rather smoothly. Still the calculation with the phase transition is not steep enough for this increase. In plasma the number of degrees of freedom is large leading to a large heat capacity and slow increase of initial temperature.

There are several effects which tend to increase the calculated $\langle p_T \rangle$. The curves (*b*) and (*c*) in Fig. 17 show the effect of mass on $\langle p_T \rangle$. Also some initial transverse motion may be present. Especially for smaller nuclei, the decoupling is probably more complicated and there might be appreciable surface emission of pions at early hot stage of the collision. In addition to the overall increase of $\langle p_T \rangle$, some of these effects may steepen the curve, but none of them seems to lead to a situation where a sharp break appears. Neither does the present data show compelling evidence for such a break. It may well be that it is not possible to distinguish between different equations of state on a basis of qualitative features of data but instead a careful quantitative analysis is called for.

I would next like to discuss the possibility of thermal origin of the highest values of $\langle p_T \rangle$ ($\langle p_T \rangle > 1$ GeV) present in the data. For massless bosons in thermal equilibrium, $\langle p_T \rangle = 2.12\,T$ and $\langle E \rangle = 2.70\,T$. (For plasma at critical temperature these values are, due to the contribution from vacuum energy, increased roughly by a factor of 4/3. Above T_c the thermal energy soon dominates.) Disregarding the mass effects, the number of particles (in any comoving volume) cannot decrease during the expansion becaus eentropy cannot decrease. In the case of a spherical system, if the entropy production in the expansion is not large, the final value of $\langle E \rangle$ (and $\langle p_T \rangle$) equals roughly the initial value and gives directly the initial temperature.

In the boost invariant case the relevant comoving volume corresponds to a fixed rapidity interval, and this volume will lose some of its energy into the longitudinal expansion. At early stage of the expansion, when the transverse motion is weak, this leads not

only to smaller values of $\langle E \rangle$ but also of $\langle p_T \rangle$. Consequently the final $\langle p_T \rangle$ is smaller than the thermal $\langle p_T \rangle$ corresponding to the initial temperature T_i. (At $T_i \simeq T_c$, the vacuum energy contribution leads to values of $\langle p_T \rangle > 2.1\, T_c$. Here we are concerned with large $\langle p_T \rangle$'s and T_i's and the vacuum energy contribution can be disregarded.) This would also hold for the Landau type initial conditions because then due to the smaller dimension of the system in the longitudinal direction, the longitudinal motion will build up faster and gain more of the energy than the transverse motion. We thus arrive to a lower bound for the initial temperature in terms of the measured $\langle p_T \rangle$ of the pions:

$$T_i \geqslant \frac{\langle p_T \rangle}{2.1}, \tag{8.2}$$

where equality holds approximately for spherical case and T_i is well above the bound for boost invariant and Landau initial conditions.

If the JACEE data is interpreted to originate from a state where matter at early stage of the collision is in approximate thermal equilibrium, the above bound indicates that initial temperatures

$$T_i > 500 \text{ MeV} \tag{8.3}$$

are reached in the events with highest values of $\langle p_T \rangle$. As an example let us consider the Ar + Pb event at $E = 1.0$ TeV/n with $\langle p_T \rangle = 1.2 \pm 0.2$ and $dN/d\eta = 134 \pm 8$ [28]. This certainly should be enough for the formation of plasma. However, such a high initial temperature of plasma implies very high values of initial energy and particle densities, $\varepsilon_i \geqslant 100$ GeV/fm^3 and $n_i \geqslant 60$ fm^{-3}, which do not seem to be compatible with the data. With the boost invariant initial conditions, $dN/dy \propto \tau_i T_i^3$ and can in principle be made arbitrarily small by taking a small enough τ_i. For the multiplicity to be compatible with the high initial densities, all the matter per unit rapidity should originate from a volume which is less than 3 fm^3 at τ_i. Together with the transverse area ~ 40 fm^2 for the Ar nucleus this leads to a very small value for τ_i. However, since the temperature drops very fast at the early stage due to the longitudinal cooling, it is not T_i but T at $\tau \geqslant 1$ fm which is relevant for the final value of $\langle p_T \rangle$. With Landau initial conditions the thickness of the original pancake would be $\leqslant 0.2$–0.3 fm for the total multiplicity not to exceed the experimental value. With such a large asymmetry in the initial conditions one would again expect the final $\langle p_T \rangle$ to be well below $2T_i$.

One possibility is that the initial state consists of separate hot spherical fluctuations. From uncertainty relation one would expect that the temperature and the radius of these fluctuations satisfy

$$r = \frac{\kappa}{T_i}, \quad \kappa \sim 1. \tag{8.4}$$

For plasma with T_i clearly above T_c the average number of quanta in such a fluctuation is then

$$N_{fl} = \frac{4\pi}{3} r^3 \frac{4a_q}{c} T_i^3 \simeq 4a_q \kappa^3 \sim 20 \tag{8.5}$$

(independent of T_i). In the above JACEE event this would mean that on the average ~ 10 fluctuations per unit rapidity with $T_i \sim 500$ MeV and radius ~ 0.4 fm would take place and produce the main part of the particles, because the measured $\langle p_T \rangle$ refers to all particles in an extended rapidity interval. Such a picture where particles are produced from independent well separated hot spots, even though possible, does not sound as the most probable.

To summarize this Section, if the high values of $\langle p_T \rangle$, observed by the JACEE group, are assumed to have a thermal origin, they indicate initial temperatures, $T_i \sim 500$ MeV or even higher. According to the standard interpretation, these are high enough for the production of QCD-plasma. This interpretation, however, may not be compatible with the observed multiplicities, because the large number of degrees of freedom in the plasma indicates much higher multiplicities (by a factor ~ 10 in our calculation) than the measured ones. Otherwise a rather peculiar concentration of the production into initial well separated hot spots is needed.

9. Effects of flow on dilepton spectra

Once the thermal space-time history of the collision is known, the amount of dilepton emission from the collision can be calculated by folding the thermal emission rates from different phases with the flow. In the mixed phase, the system is assumed to emit independently both from the plasma and the hadron phase, the relative amounts being fixed by the entropy ratio. The main difference of the dilepton signal as compared to the p_T-distributions of hadrons is, that the signal now depends on the whole space-time volume of the event. Among other things this means that τ_i and T_i are important separately, because emission is strongly temperature dependent.

The emission rate from plasma is simply (for $q\bar{q} \to l^+l^-$)

$$\frac{dN}{d^4x dM^2 d^3\vec{p}/E} = \frac{\alpha^2}{8\pi^4} \sum e_q^2 e^{-E/T}. \tag{9.1}$$

The calculation of the emission rate from the hadron gas is more complicated [45]. Since we assume the hadron gas to be dominated by the pions, we include only the process $\pi^+\pi^- \to l^+l^-$. The emission rate is then

$$\frac{dN}{d^4x dM^2 d^3\vec{p}/E} = \frac{\alpha^2}{8\pi^4}\left(1 + \frac{2m_l^2}{M^2}\right)\left(1 - \frac{4m_\pi^2}{M^2}\right)\frac{F^2(M)}{12} e^{-E/T}, \tag{9.2}$$

where $F^2(M)$ is the pion form factor. This could be taken from pion production data in e^+e^- annihilations, but in principle finite temperature effects [46, 47] may cause modifications. We are mainly interested in the qualitative differences between the emission spectra from plasma and hadron phases and in seeing how the flow can change them. For matter at rest, not only the high mass but also the high p_T pairs are dominated by the high temperature plasma, whereas the low mass pairs may exhibit clear resonance structure coming

from the hadron gas. For simplicity we include in $F^2(M)$ only the rho pole:

$$F^2(M) = \frac{m_\varrho^4}{(m_\varrho^2 - M^2)^2 + m_\varrho^2 \Gamma_\varrho^2}, \tag{9.3}$$

with $m_\varrho = 0.77$ and $\Gamma_\varrho = 0.155$ GeV. The change of the parameters of the rho meson in the hadron gas [46] is an interesting problem which might be observed in the experimental dilepton spectra. It would not, however, change qualitatively the effect of flow, which I will describe here. For small mass pairs, $M \leqslant 2m_\pi$, the bremsstrahlung will certainly give an important contribution.

Writing

$$d^4x = \tau d\tau d\eta r dr d\phi \tag{9.4}$$

in the convolution integrals over the flow, the η and the ϕ integrals can be done (see the decoupling integrals) leading to the form

$$\frac{dN}{dM^2 dy d^2 p_T} = \frac{\alpha^2}{2\pi^3} \int \tau d\tau r dr I_0\left(\gamma_r v_r \frac{p_T}{T}\right) K_0\left(\gamma_r \frac{M_T}{T}\right)$$

$$\times \left\{ \sum e_q^2 \Theta(Q) + \left[\frac{\varepsilon - \varepsilon_H}{\varepsilon_Q - \varepsilon_H} \sum e_h^2 + \frac{\varepsilon_Q - \varepsilon}{\varepsilon_Q - \varepsilon_H} G(M) \right] \Theta(M) + G(M)\Theta(H) \right\}, \tag{9.5}$$

where the Θ-functions give the regions of different phases and

$$G(M) = \tfrac{1}{12} F^2(M) \left(1 - \frac{4m_\pi^2}{M^2}\right).$$

This result can still be integrated analytically over the transverse momentum of the emitted dilepton pairs giving the mass distribution of the pairs:

$$\frac{dN}{dM^2 dy} = \frac{\alpha^2}{\pi^2} \int \tau d\tau r dr M T K_1\left(\frac{M}{T}\right) \{\ldots\}. \tag{9.6}$$

If we neglect the radial flow, the integration over r becomes trivial leading to simple single integrals for the spectra which I will not write down here [4]. With the flow the remaining double integrals must be performed numerically.

The resulting p_T–distributions at (almost) the rho peak, $M = 0.8$ GeV, are shown separately for each phase in Fig. 18 as a function of the transverse mass both with (solid lines) and without (dashed lines) the transverse flow for $T_i = 500$ MeV at $\tau_i = 0.5$ fm. Note, that the quark phase contribution does not depend separately on mass M and transverse mass $M_T = \sqrt{p_T^2 + M^2}$ and that the mixed and hadron phase contributions have their largest values at the rho peak. Even at $T_i = 500$ MeV the flow of the quark phase is weak and the two cases do not differ much for the quark phase. For the mixed phase and especially for the hadron phase the effect of the flow is very large. As indicated in the figure, the exponential slope for the latter changes from -6 to -2. With flow, the

production of high M_T pairs (at this mass value) is as effective from the mixed and hadron phase as from the quark phase. For the latter it happens because of the high temperature, and it does not matter if the pairs have small mass and high p_T or large mass but small p_T. For the former the production of large mass pairs is suppressed, since the temperature is relatively low, but small mass pairs can acquire large M_T form of the transverse flow.

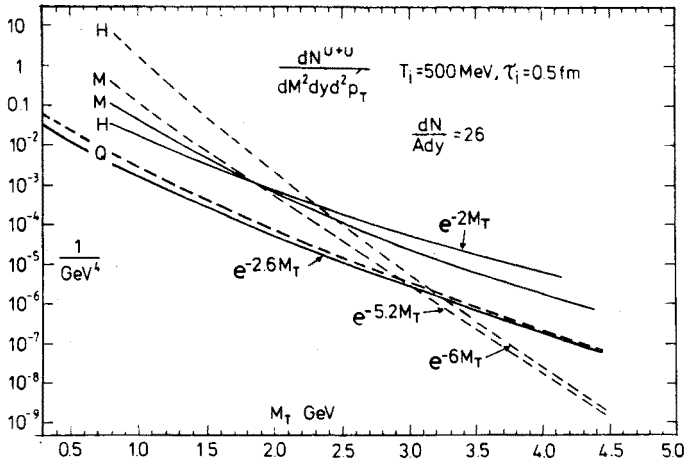

Fig. 18. Dilepton distributions as function of transverse mass for $M = 0.8$ GeV. Contributions from plasma (Q), mixed phase (M) and hadron gas (H) are shown separately both with (solid lines) and without (dashed lines) transverse flow

In Fig. 19 the distributions are plotted for different fixed values of M_T as a function of M. Without flow the low temperature phases (M and H) cannot produce high transverse masses. The result would be the extinction of the rho peak [48] as shown in Fig. 19a, when the mass spectrum is plotted for larger and larger M_T. With flow, the ϱ peak may even increase in relative strength. Its observation at large M_T would be direct evidence of the existence of collective motion of the hadronic matter produced in high energy nuclear collisions.

I will next discuss the effect of the initial temperature on the dilepton spectra. As was argued above, changing τ_i and T_i does not change much the flow as long as $\tau_i T_i^3$ stays constant. In Fig. 20 the mass spectra of dileptons from the quark phase are shown for three different T_i but same value of $\tau_i T_i^3$. The mixed and hadron phase contributions are shown only for $T_i = 500$ MeV, since the two other cases are almost identical. As is expected, the high mass part of the spectrum depends quite sensitively on the initial temperature (or equivalently time). It is this part of the spectrum, which can offer the possibility to diagnose the plasma. However, one should be cautious, because the nonthermal background is badly known and may eventually hide this effect. A rough estimate of the Drell-Yan part of the background is indicated in Fig. 20. It seems to fall safely below the thermal rates, but one should note that the Drell-Yan production is independent of multiplicity whereas the thermal production depends strongly on it [4] and that high enough multiplic-

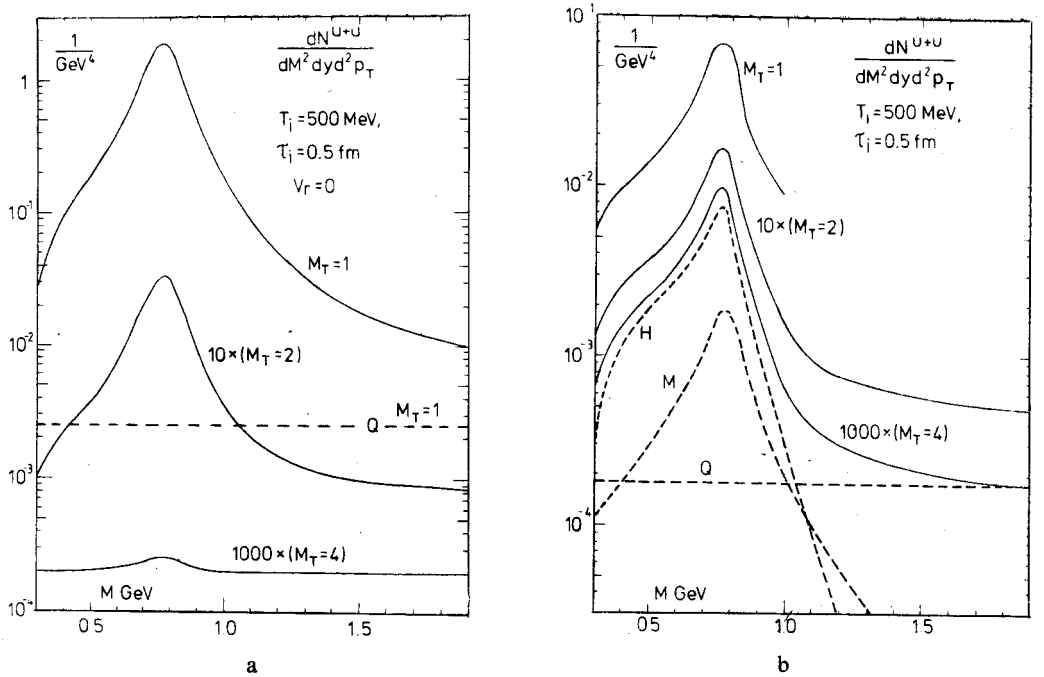

Fig. 19. Dilepton spectra as a function of the invariant mass of the pairs for different fixed values of transverse mass (a) without and (b) with transverse flow

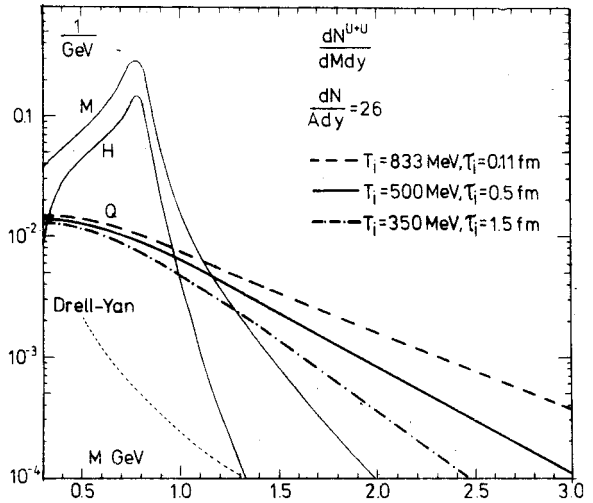

Fig. 20. The effect of initial temperature (and time) on dilepton spectra for fixed hadronic multiplicity. Low temperature phases (M and H) are essentially independent of T_i but the change of the high mass part of the plasma component (Q) is appreciable

ities may not occur in actual collisions. Dileptons may also be emitted during the pre-equilibrium stage between the primary collision and the thermalization time and in a specific model [49] this emission has been shown to be quite abundant for the high mass pairs. A better understanding of the dilepton backgrounds is really crucial for firmer conclusions on the plasma diagnostics through the dileptons of high invariant mass.

10. Processing of strangeness during hydrodynamic evolution

Strangeness is often considered as one of the favorite signals for quark matter [7]. In order to draw any conclusions on strangeness, it is necessary to follow the evolution of the strangeness abundance through the evolution of the produced matter. Depending on the timescales of the strangeness equilibration, it may also be necessary to know how abundant is the strangeness production. For the evolution we will adopt the following very simple procedure: We assume that the hydrodynamics is not affected by strangeness but can be calculated first using the bag equation of state as described earlier. (See the arguments in the connection of p_T–distributions of kaons and nucleons). In the plasma phase, we have included the strangeness by half weight as compared to the light quarks and the effect of any realistic deviation from this on the bag equation of state cannot be large.

As for the initial conditions in the CR with (almost) zero baryon number, it seems natural to assume that $n_s \simeq n_s^{eq}$, the equilibrium density. For $T_i \gg m_s$ this must clearly be the case and then all quarks have roughly the same abundance. (In [50] n_s is taken to be zero, initially). A good measure of the strangeness abundance is the ratio to the entropy, since the approximately conserved total entropy can be determined by measuring the multiplicity, $dN/dy \simeq (dS/dy)/3.6$. In equilibrium plasma $n_s/n_{tot} \sim 10\%$ using the ideal gas formulas. This is not very large because a large part of the entropy is in the form of the gluons. However, the expansion and the phase transition change the system in such a way that the initial amount of strangeness will not correspond to the equilibrium abundance at the later times. The final signal then depends on how the strangeness changing reactions will process the strangeness abundance from τ_i to the decoupling.

The kinetic equation, which describes this processing, is

$$\begin{aligned} \partial_\mu(nu^\mu) &= u^\mu\partial_\mu n + n\partial_\mu u^\mu \\ &= R_{gain} - R_{loss}, \end{aligned} \tag{10.1}$$

where R's are the appropriate rate terms for strangeness changing processes, $s\bar{s} \to q\bar{q}$, gg in quark matter and $K\bar{K} \leftrightarrow n\pi, \ldots$ in the hadron gas. The total strangeness density is

$$n = (1-h)n_s + hn_K, \tag{10.2}$$

with $n_K = n_{K^-} + n_{\bar{K}^0}$ and h, the fraction of hadron gas which is zero in the quark phase, one in the hadron phase and given by (6.3) in mixed phase. The term $u^\mu\partial_\mu n$ in (10.1) expresses the change of n in the comoving frame and $n\partial_\mu u^\mu$ gives the effect of the increase of volume in the expansion.

The collision terms have been estimated by several authors [50–52] and there is some

discrepancy in the results [51]. The form of the rate terms which we have used is that of Ref. [50] (somewhat simplified) but we have varied the strength. I will not describe them here [4], because they are not very crucial for the conclusions. Instead, let me note that due to the finite mass of the strange quarks and the kaons, the strangeness density tends to grow relative to the equilibrium density when the matter expands. In the quark phase $m_s < T$ (we have taken the strange quark mass to be 150 MeV) and the effect is not large. E.g. if $T_i = 500$ MeV and n_s starts from the equilibrium value initially, it will be only $\sim 10\%$ above the equilibrium value at $T_c = 200$ MeV even if the rate terms are neglected. In Ref. [51] the strangeness equilibration time is estimated to be <4 fm for $T > 300$ MeV. Other estimates are even shorter. For high multiplicities the plasma life time τ_Q is longer, allowing the strangeness to reach approximate equilibrium density at T_c regardless of the initial abundance. One can then conclude that the strangeness density in the central region will very likely be close to its equilibrium value when the quark phase has cooled to T_c.

Even with rate terms given, Eq. (10.2) does not yet specify completely the strangeness evolution in our model with phase transition. In the phase transition the quark-gluon degrees of freedom are bound to pions and kaons. In the smooth scenario which we use, this happens so that the volume of the matter increases by the factor $r_{dof} = g_q/g_h$. Consequently, the strangeness density n is reduced by the same factor $r_{dof} \sim 14$ if the phase transition itself does not create or destroy strangeness. This ratio should be compared to the ratio of equilibrium densities, $r_{eq} = n_s^{eq}(T_c)/n_K^{eq}(T_c)$, which is 6.5 at $T_c = 200$ MeV and 8.1 if $T_c = 160$ MeV. It follows from these numbers, that the hadron phase comes out from the phase transition with n_K below the equilibrium value by roughly a factor of two, if strangeness is not produced in the transition.

The above conclusion seems at first somewhat surprising because it indicates that the less massive s-quarks are less abundant than the heavier K-mesons [53, 50]. The reason to this is that the expansion is determined by the entropy of the system and due to this fact the strangeness to entropy ratio, n/s and not n as such, is the essential measure of the strangeness. (Remember definition (10.2).) In hadron phase, even with the large kaon mass, the four kaon states take a relatively large part of the total entropy, which they have to share only with the three pion states. In quark matter on the other hand, s-quarks have to share the entropy, in addition to the two light quark species, also with gluons. Since for a given total entropy the volume is inversely proportional to the entropy density, the total number of strange particles is proportional to n/s and at the same temperature kaons win.

In mixed phase we have two densities n_s and n_K and so far only one equation, (10.1). In our scenario the expansion in the mixed phase is completely due to the increase of the low entropy-density hadron fraction as the matter is converted from plasma to hadrons. In a volume element of plasma with no conversion, there is no expansion. This means, if we assume that there is no strangeness transfer between the two phases other than through the phase conversion, that the density of strange quarks, n_s, satisfies Eq. (10.1) without the volume expansion term $n_s \partial_\mu u^\mu$. Since h is given by the hydrodynamics, we now have a closed system of equations also in the mixed phase.

As I explained above, under the assumptions which we have done, n_K is roughly half of its equilibrium value as the matter is converted to hadrons. How much closer to n_K^{eq}

it gets in the mixed phase depends on the size of the rate terms which determine the relaxation time. An example of the numerical results with $T_i = 500$ MeV at $\tau_i = 0.5$ fm is given in Fig. 21, where the space-time dependence of strangeness is shown as contour curves of the ratio n/n^{eq}. The thick lines are the borders of the mixed phase and the dashed-dotted curve gives the decoupling surface which we used for hadron distributions. The most dramatic feature in this figure is the sudden rise of the ratio in the hadron phase. This is the consequence of the transverse flow which in the hadron phase is strong enough to

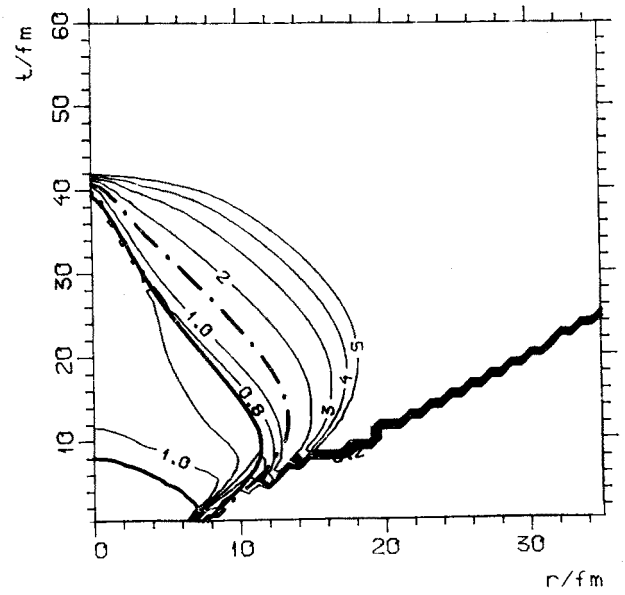

Fig. 21. Ratio of the calculated strangeness density to the equilibrium density. Thick lines are the borders of mixed phase and the dashed-dotted line is the decoupling boundary

lead to the freeze out of the strangeness changing reactions. Consequently, the final strangeness abundance is fixed in the mixed phase at T_c. This is actually a nice feature because the decoupling temperature is not a very precisely defined quantity. If the strangeness abundance could stay close to the equilibrium value in the hadron phase, it would be much more difficult to estimate the final amount of kaons.

If the same calculation is repeated with the hadron rate term reduced by a factor of 10, the ratio drops around 0.6 at the end of the mixed phase. This is a factor of 1.5 less than the result of the first calculation and is the source of the main uncertainty in this scheme. In the latter case the abundance would be very close to the equilibrium density at $T_{dec} = 140$ MeV.

Since different parts of the system decouple at different times, the strangeness density will vary along the decoupling curve. This can in principle change the shapes of the kaon p_T-distributions from those calculated in Sect. 7, where chemical equilibrium was assumed

to hold for kaons at decoupling. Actually the change of shape is not significant as is shown in Fig. 22 with distributions calculated both ways. This can be anticipated from Fig. 21 which shows that for a large part of the decoupling curve, n remains constant.

The conclusion on the strangeness signal in the CR is that it will not exhibit any clear-cut features connected with the possible plasma formation. On the contrary, in the present scenario it is most likely rather insensitive on the initial temperature if the plasma is formed in the collision, and approaches some limiting value if plotted e.g. against the

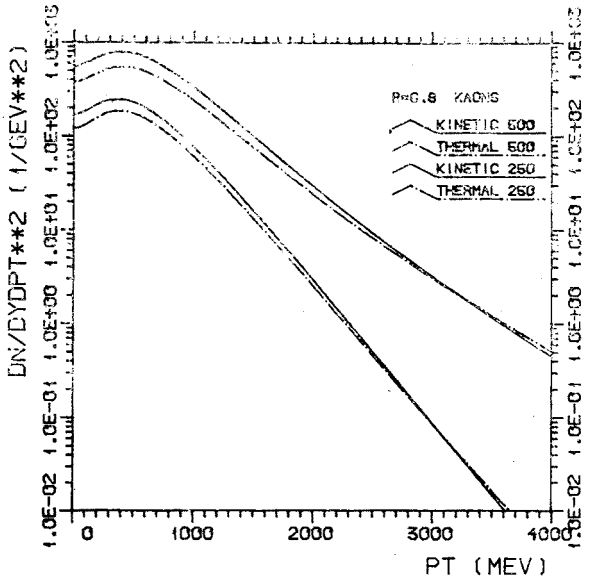

Fig. 22. Transverse momentum distribution of kaons with strangeness processing included (solid line) and assuming equilibrium density at decoupling (dashed line)

total multiplicity. This value is clearly larger than in the high energy hadron-hadron collisions and is a measure of the critical temperature T_c. How accurately the critical temperature can be determined, depends at least partly on the knowledge of the rates of strangeness changing processes in the hadron phase. Both in our case and that of Ref. [51] it is assumed that strangeness is not created in the phase transition itself. Since the number of final hadrons equals roughly (neglecting mass effects and boson-fermion differences) the combined number of quarks, antiquarks and gluons, plenty of $q\bar{q}$-pairs must be created when plasma converts to hadrons. There is actually no reason to assume that no $s\bar{s}$-pairs would be among them and even with large suppression, they would bring the strangeness closer to the equilibrium density at the end of the mixed phase making the determination of T_c even more plausible. Anyway, a better knowledge of the strangeness changing processes, especially in the hadron phase would be desirable.

11. Summary and outlook

I have presented a scenario for the calculation of several experimentally measurable quantities in the CR of ultrarelativistic nuclear collisions. It is based on the assumptions that the produced matter is sufficiently dense and smooth and the system is sufficiently large for the application of thermodynamics and hydrodynamics to the description of the major part of the multiple interactions among the produced quanta and their effects on the observable quantities. For the calculation of observables a minimum amount of kinetic considerations is used in constructing a decoupling algorithm and to obtain the rates for dilepton emission and strangeness processing. If our hopes to see the plasma are realistic, these assumptions should be reasonable ingredients in the description of nuclear collisions. In addition, several specific assumptions concerning e.g. the equation of state and the phase transition kinetics which may or may not be true, must be done. We think that our results are somewhat more general than these specific assumptions and give the gross features of the collision if the evolution of the matter proceeds smoothly. E.g. strong supercooling is excluded but we would not expect the results for a sharp second order phase transition or for the Van Hove scenario [38], where the matter breaks to plasma droplets at critical temperature, to deviate essentially from the results presented here.

Another crucial assumption is that the initial spatial fluctuations are not dominant or will dissipate out soon in the course of the collision. Equally well it may happen that they tend to lead to instabilities of the flow which destroy the cylindrical symmetry. Such behaviour may lead to interesting signals but, like phenomena connected with supercooling of plasma, they cannot be treated with the methods presented here.

Even with all these reservations we feel that the results are encouraging. They show interesting correlations among measurable quantities, like the multiplicity and transverse momentum, which reflect the properties of the strongly interacting matter at various stages of the collision. Observation of collective flow, which should show up independent of the phase transition scenarios, if high initial densities are reached, should be possible through the measurement of transverse momenta of hadrons of different mass as well as of dilepton pairs in the rho mass region. It might be possible to obtain information on temperatures at different stages of the collision from the properties of the dilepton spectra and the final strangeness abundance.

There are several points which can be pursued further. A more realistic equation of state is on the easier side and obtaining solid information on the transition kinetics on the more difficult side. Hydrodynamics may work for a large part of the evolution but at both ends of the hydrodynamic era kinetic considerations are essential. For high mass dileptons, which seem to be the most direct link to the very early stages of the collision, this is absolutely crucial. A better treatment of the decoupling stage would give more confidence on the hadron spectra. Finally, a truly 1+3-dimensional (with cylindrical symmetry) calculation is necessary for estimating the fragmentation regions. It would also, most probably, reveal interesting couplings between the transverse and longitudinal collective motions.

As a final comment I should like to notice the great importance of the coming ex-

periments at CERN and BNL. They may not be at high enough energy or with heavy enough nuclei for the production of sufficiently dense matter for plasma formation, but they will certainly be very valuable in getting a better hold on production phenomenology and, more generally, in helping to assess which of the present ideas are worth of being pursued further and which are the ones to be disregarded.

I should like to thank the organizers for the warm hospitality during the school. It has been a great pleasure and much fun to work with my collaborators.

REFERENCES

[1] H. von Gersdorff, M. Kataja, L. McLerran, P. V. Ruuskanen, *Phys. Rev.* **D34**, 794 (1986).
[2] B. L. Friman, K. Kajantie, P. V. Ruuskanen, *Nucl. Phys.* **B266**, 468 (1986).
[3] M. Kataja, P. V. Ruuskanen, L. McLerran, H. von Gersdorff, *Phys. Rev.* **D34**, 2755 (1986).
[4] K. Kajantie, M. Kataja, L. McLerran, P. V. Ruuskanen, *Phys. Rev.* **D34**, 811 1986).
[5] M. Kataja, K. Kajantie, P. V. Ruuskanen, *Phys. Lett.* **79B**, 153 (1986).
[6] For a review, see Quark Matter '84, Proc. Fourth Int. Conf. on Ultrarelativistic Nucleus-Nucleus Collisions, ed. K. Kajantie, Springer, 1984.
[7] B. Müller, *The Physics of the Quark-Gluon Plasma*, Lecture Notes in Physics **225**.
[8] J. Cleymans, R. V. Gavai, E. Suhonen, *Phys. Rep.* **130**, 217 (1986).
[9] H. Satz, *Ann. Rev. Nucl. Part. Sci.* **35**, 245 (1985).
[10] J. Kogut et al., *Nucl. Phys.* **B225** [FS9], 93 (1983).
[11] B. Berg, J. Engels, E. Kehl, B. Waltl, H. Satz, *Z. Phys.* **C31**, 167 (1986).
[12] J. Engels, H. Satz, *Phys. Lett.* **159B**, 151 (1985).
[13] A. Capella, C. Pajares, A. V. Ramallo, *Nucl. Phys.* **B241**, 75 (1984).
[14] H. Sumiyoshi, S. Date, N. Suzuki, O. Miyamura, T. Ochiai, *Z. Phys.* **C23**, 391 (1984).
[15] T. S. Biro, H. B. Nielsen, J. Knoll, *Nucl. Phys.* **B245**, 449 (1984).
[16] K. Kajantie, T. Matsui, *Phys. Lett.* **164B**, 373 (1985).
[17] A. K. Kerman, T. Matsui, B. Svetitsky, *Phys. Rev. Lett.* **56**, 219 (1986).
[18] A. Białas, W. Czyż, *Phys. Rev.* **D31**, 198 (1985); *Nucl. Phys.* B, to be published.
[19] M. Gyulassy, A. Iwazaki, *Phys. Lett.* **165B**, 157 (1986).
[20] L. McLerran in Ref. [6].
[21] D. Kisielewska, *Acta Phys. Pol.* **B15**, 1111 (1984).
[22] R. C. Hwa, K. Kajantie, *Phys. Rev. Lett.* **56**, 696 (1986).
[23] G. Baym, *Phys. Lett.* **138B**, 18 (1984).
[24] G. Baym, B. Friman, J.-P. Blaizot, M. Soyeur, W. Czyż, *Nucl. Phys.* **A407**, 541 (1983).
[25] J. D. Bjorken, *Phys. Rev.* **D27**, 140 (1982).
[26] J. P. Boris, D. L. Book, *J. Comput. Phys.* **11**, 38 (1973); **20**, 397 (1976); D. L. Book, J. P. Boris, K. Hain, *J. Comput. Phys.* **18**, 248 (1975).
[27] S. T. Zalesak, *J. Comput. Phys.* **31**, 335 (1979).
[28] The JACEE Collaboration, T. H. Burnett et al., Nucleus-Nucleus Interactions above Several Hundred GeV/*n*, 19th International Cosmic Ray Conference, 1985.
[29] J.-P. Blaizot, J.-Y. Ollitrault, Saclay preprint PhT/86-39, submitted to *Nucl. Phys.* A.
[30] J.-P. Blaizot, XXVI Cracow School of Theoretical Physics, *Acta Phys. Pol.* **B18**, no 7 (1987).
[31] For a pedagogical introduction, see S. Weinberg, *Gravitation and Cosmology*, John Wiley & Sons, New York 1972.
[32] A. Białas, W. Czyż, *Acta Phys. Pol.* **B15**, 247 (1984).
[33] R. Courant, K. Friedrichs, *Supersonic Flow and Shock Waves*, Springer Verlag, New York 1976.

[34] K. Kajantie, R. Raitio, P. V. Ruuskanen, *Nucl. Phys.* **B222**, 152 (1983).
[35] P. Danielewicz, P. V. Ruuskanen, *Phys. Rev.* **D35**, 344 (1987).
[36] B. L. Friman, G. Baym, J.-P. Blaizot, *Phys. Lett.* **123B**, 291 (1983).
[37] M. Gyulassy, K. Kajantie, H. Kurki-Suonio, L. McLerran, *Nucl. Phys.* **B237**, 447 (1984).
[38] L. Van Hove, *Z. Phys.* **C21**, 93 (1983); **C27**, 135 (1985).
[39] F. Cooper, G. Fry, *Phys. Rev.* **D10**, 186 (1974).
[40] P. V. Ruuskanen, *Phys. Lett.* **147B**, 465 (1984).
[41] E. V. Shuryak, Proc. of the First International Workshop on Local Equilibrium in Strong Interaction Physics, World Scientific, Singapore 1985.
[42] G. Baym, Proc. of 6th High Energy Heavy Ion Study, LBL-16281.
[43] L. McLerran, private communication.
[44] R. Hagedorn, CERN preprint, TH.3684.
[45] G. Domokos, J. I. Goldman, *Phys. Rev.* **D23**, 203 (1981); G. Domokos, *Phys. Rev.* **28**, 123 (1980).
[46] R. Pisarski, *Phys. Lett.* **110B**, 155 (1982).
[47] A. I. Bochkarev, M. E. Shaposnikov, *Phys. Lett.* **145B**, 276 (1984).
[48] P. Siemens, S. A. Chin, *Phys. Rev. Lett.* **55**, 1266 (1985).
[49] A. Białas, J.-P. Blaizot, *Phys. Rev.* **32**, 2954 (1985).
[50] J. Kapusta, A. Mekjian, *Phys. Rev.* **D33**, 1304 (1986).
[51] T. Matsui, B. Svetitsky, L. McLerran, MIT preprint CTP 1320, 1985 and CPT 1344, 1986.
[52] J. Rafelski, B. Müller, *Phys. Rev. Lett.* **48**, 1066 (1982).
[53] K. Redlich, *Z. Phys.* **C27**, 633 (1985).